Smile, You're on Camera

Aaron Steiner

Mark Olsson

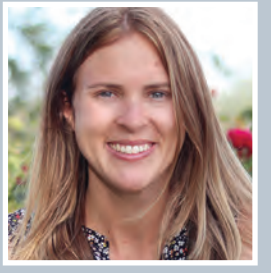

Stacey Church

Eli Perrone

Researchers discuss the development and design of deep-sea cameras.

Who should read this paper?

Marine scientists and engineers who use imaging as part of their oceanographic data collection process will benefit from reading this paper. Those interested in deep-sea imaging and its applications in oceanographic field studies will also find it of value. Subsea imaging has been used to document the deep ocean since the early 1950s, and today represents a key method for conducting oceanographic research. The camera system described in this paper not only provides high-resolution imaging at depth, but is fully autonomous and self-contained, permitting its use across a range of deep-sea vehicles and platforms for oceanographic studies. The camera's optics have been designed to correct for image distortion typically encountered with dome port optics, permitting a wide field of view with minimal vignetting, enabling researchers to visually document and inspect the seafloor and water column with minimal intervention.

Why is it important?

The camera system described here was developed over many years as a collaborative effort between DeepSea Power & Light, Woods Hole Oceanographic Institution's MISO Facility, EP Oceanographic and Ocean Imaging Systems, and Back-Bone Gear. The camera uses a unique optical design consisting of two lens elements and a high pressure-corrected dome port, which are specially configured to correct for distortion while enabling operations to depths of 6,500 m and 11,000 m. The camera's self-contained power provides >24 hours of operation for still imaging at fast repetition rates or ~18 hours for 4K or 5.3K video for continuous monitoring of deep ocean life and processes. The result is an innovative, versatile camera system that has been used on numerous research expeditions.

High-resolution imaging is a critical component of many oceanographic research initiatives happening today. Imagery captured by the camera system described in this paper has contributed to dozens of peer-reviewed publications and is a key component of ongoing oceanographic research. Furthermore, photos and videos of the deep sea engage and educate students and the public about its mysteries, fostering dialog about the ocean's importance and spurring informed decision-making.

The system is currently available and in routine use on WHOI's National Deep Submergence Facility vehicles: HOV *Alvin*, ROV *Jason*, and AUV *Sentry*. It has also been used extensively on multicorers and box corers and towed camera systems. Requests for information should be directed to D.J. Fornari at WHOI (dfornari@whoi.edu).

About the authors

Aaron Steiner is an electrical engineer by training and currently serves as the director of engineering and general manager of oceanographic products at DeepSea. Since joining DeepSea in 2010, he has developed many technologies and products focused on deep-sea imaging from LED lighting to 4K cinematographic cameras that can reach the deepest points in the world's ocean.

Mark Olsson is the founder and CEO of SeeScan, Inc., of which DeepSea is a business division representing its oceanographic product segment. In 1983, after the successful development of a pressure-compensated deep-sea battery, he founded DeepSea Power & Light to engineer and manufacture products that serve the subsea industry. Since then, he has designed numerous deep-ocean optical and lighting solutions that are used across the globe in subsea research and exploration.

Stacey Church is the communications manager at SeeScan, Inc., an original equipment manufacturer of plumbing diagnostic, electromagnetic utility location, and DeepSea oceanographic products. She joined the SeeScan/DeepSea team in 2015 as a technical writer, with a focus on creating product documentation for end users. Since then, she has authored and contributed to several articles for various industry publications on innovative technologies.

Eli Perrone was raised in West Virginia and graduated from Cornell University with a BS in science of Earth systems, with a concentration in ocean science. He spent a decade working in the commercial oceanographic survey and autonomous underwater vehicle industries before starting EP Oceanographic LLC, based in Pocasset, MA, in 2014. He focuses on the Ocean Imaging Systems underwater imaging and lighting product lines, among other pursuits.

Jon Clouter was born in Newfoundland and is a graduate of Memorial University (BFA). He has years of experience in specialized photography and 3D imaging for the visual effects industry. He is co-founder and vice president of the camera company Back-Bone in Ottawa, Canada.

Dr. Dan Fornari is a marine geologist and an emeritus research scholar in the Geology and Geophysics Department at the Woods Hole Oceanographic Institution (WHOI), and co-manager of the MISO (Multidisciplinary Instrumentation in Support of Oceanography) Facility at WHOI that specializes in development and operation of deep-sea imaging and sampling systems. His research for the past ~50 years has focused on seafloor volcanic and hydrothermal processes at mid-ocean ridges, seamounts and oceanic islands, high-resolution mapping, and sampling. He has participated in and led more than 150 research expeditions, and much of his field research has involved diving in research submersibles such as *Alvin*.

Dr. Victoria Preston is a field roboticist and assistant professor of engineering at Olin College in Needham, Massachusetts. She holds a BS degree in engineering from Olin College, and SM and PhD degrees in autonomous systems from the Massachusetts Institute of Technology and Woods Hole Oceanographic Institution Joint Program. Her research, at the intersection of autonomy and spatiotemporal modelling in marine environments, focuses on developing robots as perceptive intelligent partners for performing scientific ocean exploration.

Mae Lubetkin is an independent researcher with expertise in marine geosciences, subsea imaging, and critical media studies.

Jon Clouter

Dr. Dan Fornari

Dr. Victoria Preston

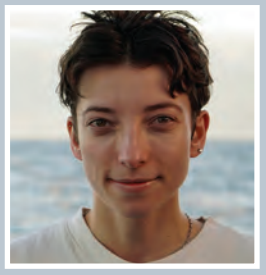

Mae Lubetkin

AUTONOMOUS, FIXED-FOCUS, HIGH-RESOLUTION DEEP-SEA CAMERA SYSTEMS

Aaron Steiner[1], Mark Olsson[1], Stacey Church[1], Eli Perrone[2], Jon Clouter[3], Daniel Fornari[4], Victoria Preston[5], and Mae Lubetkin[6]

[1]DeepSea Power & Light, San Diego, CA, USA

[2]EP Oceanographic, LLC and Ocean Imaging Systems, Pocasset, MA, USA

[3]Back-Bone Gear Inc., Kanata, Ontario, Canada

[4]Woods Hole Oceanographic Institution, Geology and Geophysics Department and MISO Facility, Woods Hole, MA, USA; dfornari@whoi.edu

[5]Northeastern University, Department of Electrical and Computer Engineering, Boston, MA USA

[6]Independent researcher, Paris, France

ABSTRACT

The development and design of versatile, autonomous, fixed-focused deep-sea cameras capable of operation to depths of 6,000 m and 11,000 m, that have been deployed on numerous research submersibles and deep-sea platforms since 2016, is presented. The optical assembly of the cameras consists of two lens elements and a high pressure-corrected dome port, optimized to correct for image distortion, produce minimal vignetting, and yield a depth of field which extends from ~0.5 m to infinity within the subsea environment. Three configurations of deep-sea housing are integrated with these optics, such that the internal chassis designs permit GoPro HERO4™ and HERO11™ camera modules to be axially aligned with the corrector and dome optics. The GoPro cameras are fitted with a 5.4 mm non-distortion lens and 1TB microSD memory cards; and are connected to a high-capacity USB-C battery or custom Li-battery pack to provide self-contained power. The supplemental power and recording media storage permit operations for >24 hours for 27MP still imaging at a high (~5 second) repetition rate, or ~18 hours for 4K or 5.3K cinematic video acquisition at 30 fps. The self-contained power and autonomous design of these cameras allow a wide range of installation options for deep-sea vehicles, towed systems, and seafloor sampling devices to document oceanographic processes. In addition to their use for high-resolution documentation of Earth-ocean phenomena and life, they have been used in numerous outreach efforts to educate and engage students and the public about the importance of continued exploration and study of "inner space" – the global ocean and seafloor.

Keywords: Deep-sea cameras; Fixed-focus; Deep-submergence research; Versatility in subsea imaging systems; Subsea depth of field

INTRODUCTION

Milestones and Background in Deep-sea Imaging Technologies

The first underwater camera was developed by British engineer William Thompson in the mid-1800s, and the first underwater filming was accomplished in 1896 by French biologist Louis Boutan. In the early 1950s, Harold Edgerton, an engineering professor at MIT, developed the first deep-sea strobe light, providing triggered, high-intensity lighting required to take photographs of the deep ocean and seafloor for the first time [1]. That development led to the first generation of deep-sea cameras through the engineering efforts of Maurice "Doc" Ewing and Lamar Worzel at the Lamont Geological Observatory as well as J. Brackett Hersey, Allyn Vine, and David Owen at Woods Hole Oceanographic Institution (WHOI) [2], [3]. Those early deep-sea camera systems were rudimentary but provided key photographic evidence of animals and seafloor features over small areas in the deep ocean. This imagery significantly expanded the knowledge of features, processes, and causal links between geological, biological, and chemical phenomena on the seafloor (e.g., see discussion and references in [4]). Early deep-sea camera systems were also crucial for deep-sea search and/or recovery missions associated with strategic operations.

From the 1960s to the 1980s, marine geological, chemical, and especially biological investigations of deep-ocean terrains relied heavily on traditional optical cameras and deep-sea strobe lighting to photograph the abyssal seafloor, providing some of the first visual documentation of the abundance and diversity of life in the deep ocean, morphology and geology of volcanic terrains on the mid-ocean ridge crest, and evidence for hydrothermal venting [5], [6], [7], [8], [9]. Bruce Heezen and Charles Hollister, in their seminal 1971 book *The Face of the Deep* [5], provided the first grand compilation of deep-sea imaging taken with the newly developed underwater cameras and strobes, and discussed the scientific implications and insights that those images provided (see also *Discovering the Deep* [4] for an updated compilation of deep-sea imagery focusing on seafloor geology and hydrothermal features). During the latter part of the 20th century, subsea imaging also played a prominent role in resource development with the advent of offshore oil and gas drilling that involve seafloor completions and pipelines, all of which required visual inspections and monitoring of the production equipment to prevent and identify potential pollution from the offshore resource extraction, transmission, and delivery processes. Today, direct visual observations of the ocean floor enabled by deep-water to full-ocean depth-capable camera systems are intimately tied to understanding the dynamic and interactive physical, chemical, and biological processes occurring there. Photographic documentation of those phenomena is crucial to quantifying those processes and understanding their impacts. Today, documentation of this type plays a key role in developing environmental guidelines and mitigating impacts from 21st century energy resource projects such as offshore wind farms.

Equally important to the development of deep-sea camera systems in the late 20th century were improvements to the quality and capacity of lighting for seafloor imaging.

Prior to the 1980s, light attenuation in water of available lighting sources generally limited deep-ocean photography to objects less than 20 m from the camera, creating a significant roadblock to large-area imaging of the seafloor [10]. In the 1980s and 1990s, new towed cameras with higher capacity strobe lighting and large film magazines were deployed for both basic seafloor geological and biological mapping along the mid-ocean ridge crest and other terrains, as well as for archaeological and search missions, such as the mission that discovered the wreck of the RMS *Titanic* [11]. These systems (e.g., ANGUS and ARGO operated by WHOI's Deep Submergence Laboratory [12], and the DeepTow system developed by Fred Spiess and colleagues at the Scripps Institution of Oceanography's Marine Physical Laboratory [6]) relied on electronic controls to trigger the cameras and strobes at specific intervals and also provided acoustic telemetry to transmit basic information such as bottom water temperature, depth, and altitude along the survey track.

The next generation of deep-sea cameras began to be developed in the mid-1990s as professional and consumer digital cameras became available, and the size of digital electronics and controls were miniaturized. The development of high-precision optics that could be manufactured to withstand the extreme pressures at seafloor depths to ~6,000 m and 11,000 m was another key technological leap. Funding agencies and oceanographic facilities of many nations recognized the need for developing functional deep-sea camera systems to further oceanographic research within their territorial waters as well as for broader investigations of global ocean and seafloor processes. In the US, the Multidisciplinary Instrumentation in Support of Oceanography (MISO) Facility was established at WHOI in the early 2000s with US National Science Foundation (NSF) support to develop and implement a wide range of seafloor and deep-ocean imaging capabilities for ocean scientists to document observations and optimize seafloor sampling [13], [14].

OVERVIEW: WHOI-MISO FACILITY DEEP-SEA CAMERA SYSTEMS

The MISO Facility is the only academic, community-wide-accessible deep-sea imaging facility available to US oceanographers for cost-effective and diverse suites of field investigations requiring deep-sea digital imaging capabilities. The primary service function of the MISO Facility (www.whoi.edu/miso) at WHOI's Shipboard Scientific Services Group (WHOI-SSSG) is to assist US investigators requiring deep-sea digital imaging and sampling capabilities for seafloor experiments and surveys conducted from research vessels in the US academic research fleet, coordinated through the University-National Oceanographic Laboratories System (UNOLS). For more than two decades, the MISO Facility has been supported by the NSF through five-year "Facility" grants as well as research grants from a variety of US federal agencies, US universities, and foreign universities and agencies. MISO focuses on providing excellent, high-resolution oceanographic data sets – primarily deep-sea digital photographic and sampling equipment with real-time imaging capabilities and subsea telemetry for serial data sensors – to a wide spectrum

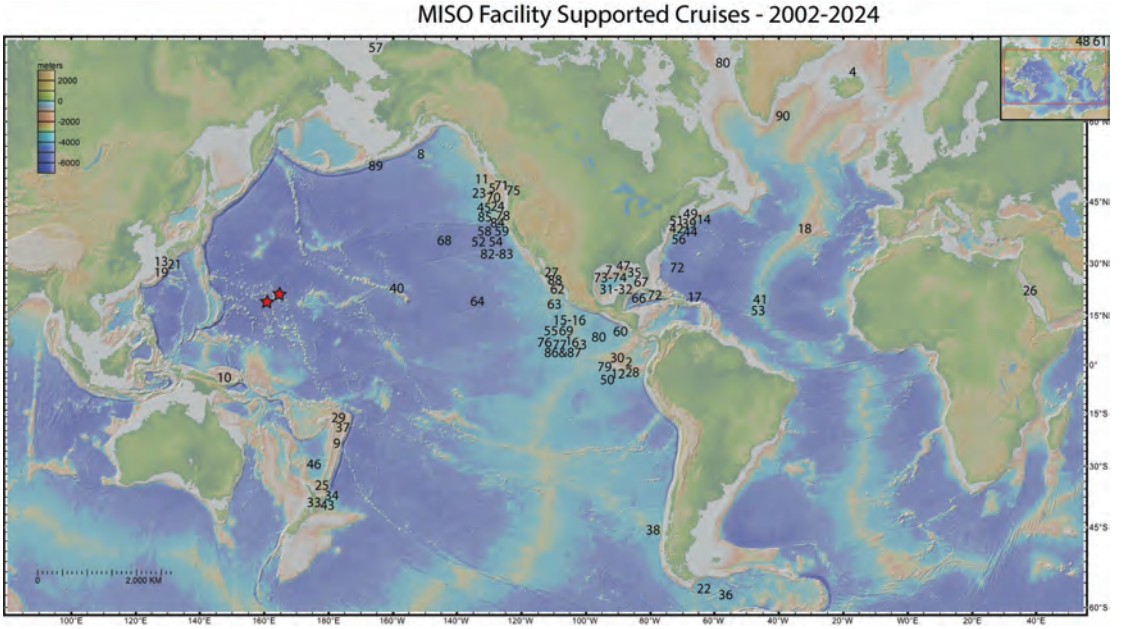

Figure 1: WHOI-MISO Facility instrumentation supported cruises (90) conducted during the period from 2002 to 2024. The cruise ID numbers are keyed to listings detailed in Table 1 that provide general location, ship name, type of deep submergence platform, official cruise ID (when known), and month/year of the expedition. Note that research cruises from approximately 2002 to 2015 utilized the DeepSea Digi SeaCam® housing with Nikon995 internal module providing 3.3MP still images using a 300-600 watt/s strobe triggered by an intervalometer in the camera electronics. Between 2015-2022, the Digi SeaCam housings have been used with a GoPro™ HERO4 internal camera module designed at WHOI-MISO, which provided 10MP still images and up to 4K video imagery at 24 fps. Since 2022, the Digi SeaCam housings have been modified with a new internal chassis to accommodate GoPro™ HERO11 cameras providing the ability to collect 27MP still images and 5.3K cinematic video at 30 fps. Since April 2024, a DeepSea Optim 11K rated housing has been modified to accommodate a HERO11 camera module that was reconfigured by Back-Bone and EP Oceanographic/Ocean Imaging Systems to provide the ability to collect 27MP still images and 5.3K cinematic video at 30 fps to full ocean depth (11,000 m), and for use with the *Alvin* research submarine to 6,500 m, its maximum operational depth. The two red stars are MISO *TowCam* surveys in the western Pacific that used deep-towed magnetometers for near-bottom geophysical surveys.

of US and foreign investigators conducting geological, biological, and chemical studies throughout the global ocean. To date, MISO has supported 90 field expeditions focused on deep-sea coral studies, benthic biology traverses and time-lapse experiments, hydrothermal vent research, mid-ocean ridge and seamount volcanism, time-series experiments in various seafloor environments, and studies of gas hydrates and related seep sites in different tectonic settings (Figure 1 and Table 1; and see Supplementary Materials).

In 2018, the MISO Facility was integrated into WHOI-SSSG, and since 2022-2023, that collaboration has expanded to include substantial interaction and joint seagoing operational efforts with Oregon State University's (OSU) Marine Rock and Sediment Sampling (MARSSAM) coring and dredging facility (M. Walzack – MARSSAM Manager). From 2022-2023, there were several opportunities for training UNOLS tech pool shipboard technicians, as well as WHOI-SSSG and OSU-MARSSAM technicians in at-sea operation and maintenance of MISO imaging and data systems. Further, MISO offers important and enabling imaging capabilities to WHOI's National Deep Submergence Facility (NDSF) vehicles (HOV *Alvin*, ROV *Jason*, and AUV *Sentry*) to improve and expand imaging capabilities for deep submergence science. Additional efforts to expand the reach and application of MISO

ID	Description	Date
1	East Pacific Rise 9° 50'N (*Atlantis* AT7-12)	May 2002
2	Galapagos Rift 86°W (*Atlantis* AT7-13)	Jun. 2002
3	Hess Deep (*Melville*)	Aug. 2002
4	Offshore Northern Iceland *(Bjarni Saemundsson*)	Jul. 2003
5	Offshore Scripps (*Sproul*)	Sept. 2003
6	East Pacific Rise 9° 50'N (*Atlantis* AT7-12)	Jan. 2004
7	Gulf of Mexico (*Pelican*)	Jul. 2004
8	Gulf of Alaska (*R. Revelle*)	Aug. 2004
9	Lau Basin (*Kilo Moana*)	Sept. 2004
10	PNG-Manam volcano (*Kilo Moana*)	Nov. 2004
11	Juan de Fuca Event Response (*T. Thompson*)	Mar. 2005
12	Galapagos Rift 86°W (*Atlantis* AT11-7)	Jun. 2005
13	Offshore Taiwan (*OR-1*)	Sept. 2005
14	New England Seamounts (*Atlantis* AT11-11)	Oct. 2005
15	East Pacific Rise 9° 50'N (*New Horizon* NH06)	May 2006
16	East Pacific Rise 9° 50'N (*Atlantis* AT15-6)	Jun. 2006
17	Puerto Rico Trench (*Pelican*)	Sept. 2006
18	Lucky Strike – MAR (*Atalante*)	Aug. 2006
19	Offshore Taiwan (*OR-1* 860)	Oct. 2006
20	East Pacific Rise 9° 03'N (*Atlantis* AT15-17)	May 2007
21	Offshore SW Taiwan (*OR-1*)	Mar. 2008
22	Drake Passage, Southern Ocean (*Palmer* NBP-08-05)	Apr. 2008
23	Axial Seamount and Hydrate Ridge (*T. Thompson* TN221)	Jul. 2008
24	Hydrate Ridge (*Wecoma* W0808)	Aug. 2008
25	S. Kermadec Seamounts, New Zealand (*T. Thompson* TN-230)	Mar. 2009
26	Red Sea, Atlantis-II Deep (*Oceanus*)	Sept. 2009
27	Guaymas Basin, Gulf of California (*Atlantis* AT15-54)	Oct. 2009
28	Galapagos Rift (*Atlantis* AT15-63)	Mar. 2010
29	Northern Lau Basin (*Kilo Moana* KM1008)	Apr. 2010
30	N. Galapagos Seamounts (*Melville* MV1007)	May-Jun. 2010
31	Gulf of Mexico (*NOAA Ship PISCES*)	Sept. 2010
32	Gulf of Mexico Time-lapse System (*Atlantis* AT18-03)	Dec. 2010
33	Lake Rotomahana, North Island, New Zealand (small boat)	Jan. 2011
34	S. Kermadec Seamounts, New Zealand (*Tangaroa*)	Feb.-Mar. 2011
35	Gulf of Mexico (*NOAA Ship McArthur II*)	Apr.-May 2011
36	Drake Passage, Southern Ocean (*N.B. Palmer*)	May-Jun. 2011
37	Lau Basin (*Kilo Moana*)	Nov.-Dec. 2011
38	Chile Ridge (*Melville*)	Apr. 2012
39	US NE Canyons (*NOAA Ship Bigelow*)	Jul. 2012
40	Hawaii – offshore Pearl Harbor (*KOK*)	Nov.-Dec. 2012
41	Mid-Atlantic Ridge 16N (*Knorr*)	May 2013
42	US NE Canyons (*NOAA Ship Bigelow*)	Jun. 2013
43	New Zealand N. Island Lakes (GNS – small boat)	Mar. 2014
44	US NE Canyons (*NOAA Ship Bigelow*)	Jul. 2014
45	Axial Seamount (*Atlantis*)	Jul.-Aug. 2014
46	Havre Volcano (*R. Revelle*) (MISO camera on ROV Jason)	Mar.-Apr. 2015
47	Svalbard 80°N (*H. Hanssen*) Multicorer w/MISO imaging	May 2015
48	Gulf of Mexico (*Pelican*) Multicorer w/MISO imaging	Jun. 2015
49	US NE Canyons (*NOAA Ship Bigelow*)	Aug. 2015
50	Galápagos Platform (*Alucia*)	Aug. 2015
51	US NE continental shelf – Mud Patch (*NOAA Ship Sharp*) MC800 Multicorer	Aug. 2015
52	California Borderland (*T. Thompson*) Multicorer	Feb. 2016
53	Mid-Atlantic Ridge 14N (*Atlantis*) TowCam, Alvin Imaging	Mar.-Apr. 2016
54	California Borderland (*Sikuliaq*) MC800 Multicorer w/MISO imaging, SVC	Mar. 2016
55	8° 20'N Seamounts – EPR (*Atlantis*), Alvin Imaging	Oct.-Nov. 2016
56	US NE cont. shelf CH_4 seeps (*Atlantis*) MC400 w/MISO imaging & Alvin Imaging	Aug. 2016
57	Chuckchi Sea (*Sikuliaq*) MC400 Multicorer w/MISO imaging	Sept.-Oct. 2016
58	California Borderland (*Sally Ride*) MC400 Multicorer w/MISO imaging	Feb. 2017
59	Monterey Canyon transect (*Oceanus*) MC800 Multicorer w/MISO imaging	Mar. 2017
60	Costa Rica Pacific Margin (*Atlantis*) Alvin with MISO GoPro imaging	May 2017
61	Svalbard 80°N (H. Hanssen-CAGE, U. Tromsø, Norway) Multicorer w/MISO imaging	Jun. 2017
62	Gulf of Calif. – Guaymas & Pescadero Basins – (*Nautilus*) MISO GoPro imaging	Oct. 2017
63	Revillagigedos Islands – (*Nautilus*) MISO GoPro imaging	Nov. 2017
64	Central Pacific Mn-nodule TowCam Surveys (*Kilo Moana*) U.Hawaii/KIOST	Mar. 2018
65	8° 20'N Seamounts & EPR 9°50'N – Early Career Training (*Atlantis*), Alvin Imaging and MISO GoPro	Dec. 2018
66	Cayman Trough- Hydrothermal (*Atlantis*) ROV Jason, MISO GoPro imaging	Jan.-Feb. 2019
67	Gulf of Mexico CH_4 seep sites (*Atlantis*) Alvin	Feb.-Mar. 2019
COVID-19 Pandemic Interrupts Oceanographic Expeditions		
68	Mid-Pacific MC800 multi-coring transect with MISO imaging on MC800 (*Kilo Moana*)	Oct. 2020
69	EPR 9° 50'N biology and geology / hydrothermal (*R. Revelle*) MISO imaging systems and high-T vent loggers on ROV Jason	Mar.-Apr. 2021

ID	Description	Date
70	Axial Seamount MISO high-T loggers on ROV Jason (*Atlantis*)	Aug. 2021
71	Hawaii & offshore Vancouver, BC, MISO GoPro imaging on ROV Hercules (*Nautilus*)	Sept. 2021
72	US SE coast and Cayman Trough, new MISO GoPro imaging from Alvin post-overhaul (*Atlantis*)	Aug. 2022
73	Gulf of Mexico methane seeps, new MISO GoPro imaging from Alvin (*Atlantis*)	Sept. 2022
74	Gulf of Mexico methane seeps, new MISO GoPro imaging from Alvin (*Atlantis*)	Oct. 2022
75	Puget Sound, MISO imaging from CTD for methane seeps (*R. Carson*)	Oct. 2022
76	EPR 9° 50'N biology, new MISO GoPro imaging from Alvin and time-lapse system (*Atlantis*)	Dec. 2022
77	EPR 9° 50'N geology & hydrothermal studies, new MISO GoPro imaging from Alvin and AUV Sentry (*Atlantis*)	Jan. 2023
78	Offshore central Oregon coast, MC800 with MISO GoPro imaging (*Sikuliaq*)	Mar. 2023
79	Galapagos Platform, deep-sea corals and geology studies, new MISO GoPro imaging from Alvin (*Atlantis*)	Mar.-Apr. 2023
80	NE Pacific transect, biogeochemistry, MISO 4K GoPro imaging on Clio AUV (*Atlantis*)	May-Jun. 2023
81	Greenland coring and multicoring, MISO GoPro and 24MP imaging on CTD and MC-800, (*Armstrong*)	Jul.-Aug. 2023
82	California Borderland & Santa Barbara Basin, new MISO GoPro cameras on Alvin (*Atlantis*)	Jul. 2023
83	California Borderland new MISO GoPro cameras on Alvin and MC400 Multicorer w/MISO 24MP imaging (*Atlantis*)	Jul. 2023
84	Hydrate Ridge MISO GoPro cameras on Alvin and 24MP downlooking camera on Alvin & MC400 Multicorer w/MISO 24MP imaging (*Atlantis*)	Aug. 2023
85	Offshore central Oregon coast, MC800 with MISO GoPro imaging (*Sproul*)	Sept. 2023
86	EPR 9° 50'N biology, new MISO GoPro imaging from Alvin and time-lapse system (*Atlantis*)	Jan. 2024
87	EPR 9° 50'N geology & hydrothermal studies, new MISO GoPro imaging from Alvin and AUV Sentry (*Atlantis*)	Feb.-Mar. 2024
88	Guaymas Basin, Gulf of California, MISO GoPro cameras on Alvin (*Atlantis*)	Apr.-May. 2024
89	Aleutian Trench, methane seeps, MISO GoPro cameras on Alvin (*Atlantis*)	May-Jun. 2024
90	North Atlantic-Greenland-Iceland, MC800 Multicorer w/MISO imaging (*Langseth*)	Jun.-Jul. 2024

Table 1: Listing of WHOI-MISO Facility Supported Cruises that utilized various deep-sea towed camera (*TowCam*) and sampling systems, and fixed focus cameras on a wide range of deep submergence vehicles between 2002 and 2024 (90 expeditions total). The cruise ID numbers are keyed to global bathymetry map shown in Figure 1. General location is provided first and then ship name in italics and official cruise ID (when known), and month/year of the expedition. Research cruises from approximately 2002 to 2015 utilized the DSPL Digi SeaCam housing with Nikon995™ internal module providing 3.3MP still images using a 300-600 watt/s strobe triggered by an intervalometer in the camera electronics. Between 2015-2022, the Digi SeaCam housings have been used with a GoPro HERO4™ internal camera module designed at WHOI-MISO, which provided 10MP still images and up to 4K video imagery at 24 fps. Since 2022, the Digi SeaCam housings have been modified with a new internal chassis to accommodate a HERO11™ camera providing the ability to collect 27MP still images and 5.3K cinematic video at 30 fps. Since 2024, a DSPL Optim 11K rated housing has been modified to accommodate a HERO11™ camera module that was reconfigured by Back-Bone and EP Oceanographic/Ocean Imaging Systems to provide the ability to collect 27MP still images and 5.3K cinematic video at 30 fps to full ocean depth (11,000 m), and for use with the *Alvin* research submarine to 6,500 m, its maximum operational depth. (Note that two cruises, TN272 in 2011 and SKQ2014S2 in 2014-2015, used a MISO *TowCam* frame and telemetry system to carry out near-bottom magnetics surveys in the far western Pacific between Hawaii and Japan {red star symbols}.)

instrumentation and capabilities to other deep submergence vehicle operators have been ongoing and successful over the past ~five years (e.g., NOAA-Ocean Exploration (NOAA-OE); Ocean Exploration Trust (OET); and Schmidt Ocean Institute (SOI)).

Scientists from the following institutions have used the WHOI MISO Towed Camera System (*TowCam*) and related MISO deep-sea imaging instrumentation over the past two decades (Figure 1 and Figure 2): Penn State U.; U. Washington; U. Hawaii; Georgia Tech.; George Mason U.; W. Washington State U.; Temple U.; Harvard U.; Lehigh U.; U. Bergen, Norway; NOAA; Smithsonian Institution; U. Tromsø, Norway; National Taiwan U.; Oregon State U.; IPGP U. Paris; KAUST; Duke U.; Navy Research Lab.; SIO; GNS New Zealand; U. New Hampshire; U. Rhode Island; UC-Santa Cruz; USGS; Stanford U.; Cal. Tech.; NOAA-OE; OET; and WHOI. Funding for these activities is provided by US federal agency grants, WHOI internal grants, and occasionally foreign research institutions and funding agencies to support science activities, technology development, and shipboard technical support.

EVOLUTION OF MISO GoPro™ DEEP-SEA CAMERA SYSTEMS

In collaboration with DeepSea Power & Light (DeepSea) (San Diego, CA), EP Oceanographic and Ocean Imaging Systems (EPO and OIS) (Pocassett, MA), and Back-Bone Canada, the MISO Facility has developed an excellent suite of autonomous, fixed focus, very high-resolution deep-sea cameras (6,000 m to 11,000 m rated) that can take >24 hrs. of 10-27MP digital still images or ~18 hrs. of 4K or 5.3K cinematic video (Figure 3). The MISO GoPro™ camera can be used on a wide range of deep-sea vehicles and sampling systems, providing an important capability to simultaneously document water column measurements, seafloor samples, and seafloor observations. The following section describes the various generations of MISO deep-sea camera systems and the ongoing collaborative efforts to produce the autonomous, high-quality system in use today.

The current iteration of the MISO deep-sea camera was developed over the past ~10 years using ~20-year-old DeepSea Digi SeaCam® camera housings originally developed to support the original MISO *TowCam* system. The *TowCam* system has provided both imaging and sampling capabilities across many seafloor environments since the early 2000s (Figure 2, Table 1) [13]. Today, the *TowCam* system primarily uses a higher resolution OIS digital still camera, which replaced the Digi SeaCam housings and the cameras they contained (3.3MP Nikon Coolpix imaging modules) in ~2012. The *TowCam* system continues to provide high-resolution (24MP) seafloor imaging using lighting provided by 300 or 600 watt/sec strobes synchronized to the camera's shutter.

In 2015, the WHOI-MISO team used off-the-shelf GoPro HERO4™ consumer cameras, with a special 5.4 mm non-distortion lens and a newly designed internal chassis that fit the older Digi SeaCam housings, including a USB-C battery pack for supplemental power, to implement a new, self-contained/autonomous deep-sea camera that could be used on a wide

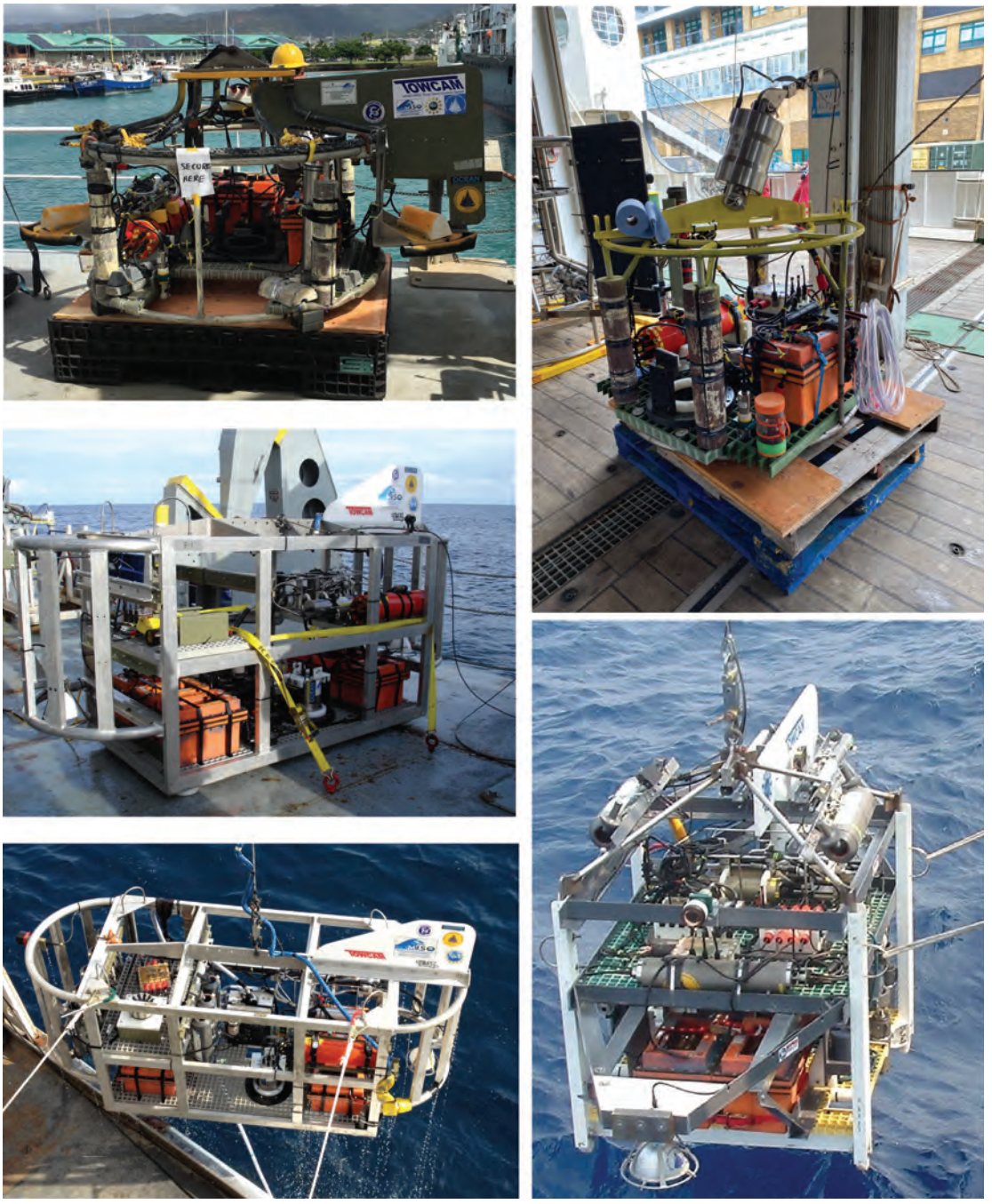

Figure 2: Examples of various configurations of the WHOI-MISO *TowCam* system capable of deep-sea imaging and sampling to 6,000 m depth (see Figure 1 and Table 1; http://www.whoi.edu/miso). *TowCam* comprises an internally recording digital deep-sea camera system (24-megapixel Ocean Imaging Systems (OIS) cameras synched to high-intensity strobes (300 or 600 watt/s). When required *TowCam* can trigger 5 litre Niskin bottles in conjunction with CTD water properties data. The *TowCam* is towed at ~1/4-1/2 knots on a standard UNOLS 0.322" coaxial CTD sea cable or coaxial cable, often with a USBL beacon to provide accurate subsea navigation, while taking photographs every ~5-10 sec. Real-time acquisition of digital depth and altitude data at 1 Hz is made possible using a Valeport 500P altimeter/depth sensor. Those data are used to help "fly" the camera using winch pay-out at ~4-5 m altitude during the tow and quantify objects in the digital images and make near-bottom profiles. Obstacle avoidance is done using a forward-looking altimeter. Two high-intensity green lasers are used to provide scale (20 cm) within the image area to help quantify the size of seafloor features. A high-speed "Data Link" system permits real-time transmission of the low-resolution video grabs from the camera display up the CTD cable to allow real-time observations of the seafloor during each bottom traverse and to help guide imaging and sampling. Full resolution images are downloaded from the camera after each dive and provided to the science team. All system components operate at 24 VDC, with power supplied by two DeepSea SeaBatteries rated at ~40 amp/hr.

Figure 3: MISO GoPro™ camera systems, 1st and 2nd generation cameras that use GoPro HERO4™ imaging modules. Left panel shows the 1st generation system in the DeepSea Digi SeaCam housing and right panel shows the 2nd generation cameras in the DeepSea Super SeaCam housing, both rated to 6,000 m operating depths.

range of deep-sea vehicles and sampling systems to document observations, samples, and vehicle operations when used on MISO designed imaging seafloor landers. Since 2015, these MISO GoPro deep-sea cameras have provided superb imaging capabilities on 30 research cruises using deep-submergence vehicles, *TowCam*, box corers and multicorers, and seafloor landers (Figure 3).

In 2018, because of the advanced age and limited availability of only three of the original MISO Digi SeaCam housings manufactured in 2002, three new DeepSea Super SeaCam housings, made out of Titanium (Ti), were purchased with National Science Foundation – Ocean Instrumentation Program funding. A collaboration between MISO and OIS led to the design and successful use of the new Super SeaCam housings with HERO4™ cameras as a "2nd generation" MISO GoPro deep-sea camera system. The Super SeaCam housing uses the exact dome and internal corrector optics as the original DeepSea Digi SeaCam housing. However, because of the internal dimensions of the Super SeaCam housing, the HERO4™ camera orientation and lens configuration required a re-design of the internal camera chassis using lens relocation hardware designed by Back-Bone Canada. OIS designed and assembled the internal chassis using HERO4™ cameras with the special 5.4 mm non-distortion lens. OIS also designed and provided an internal Li-ion battery pack

Figure 4: 3rd generation MISO GoPro™ camera system which uses a GoPro™ HERO11 camera module in a new (2024-manufacture) DeepSea Digi SeaCam housing (6,000 m rated). Left panel shows two views of the new housings. Right composite image shows the internal chassis that holds the HERO11 camera and aligns it to the housing optics, internal USB battery and cabling and associated components. Installation of the HERO11 and USB battery and set-up of the camera pre-dive takes ~15 minutes. When the camera is deployed on a vehicle in hot, tropical weather, care must be taken to cool down the housing so that the camera module does not overheat – this is especially true for 5.3K or 4K video recording.

and DC/DC converter to match the HERO4's power requirement for extended duration image acquisition (Figure 3).

The MISO-OIS GoPro™ 2nd generation deep-sea cameras in the MISO Facility continue to be used for a wide range of seafloor imaging and are requested routinely by many investigators; however, the HERO4™ cameras are no longer manufactured or supported by GoPro™, and the lens conversion kits required to support the OIS-design for the GoPro to function in the Super SeaCam housing are also not available. While the MISO facility has several spare internal chassis for this 2nd generation MISO GoPro camera, it was clear that a transition to the newer, more capable GoPro HERO11™ camera modules was needed. This upgrade in camera capabilities would continue to provide autonomous, self-contained high-resolution imaging capacity for the broad spectrum of seafloor sampling and documentation of observations required when using NDSF and other deep-submergence vehicles as well as to provide correlative seafloor images during bottom sampling using box corers and multicorers.

The 3rd generation MISO GoPro™ deep-sea cameras that utilize GoPro HERO11™ camera modules have now been used continuously on >80 *Alvin* dives since August 2022 (Figure 4). These cameras provide

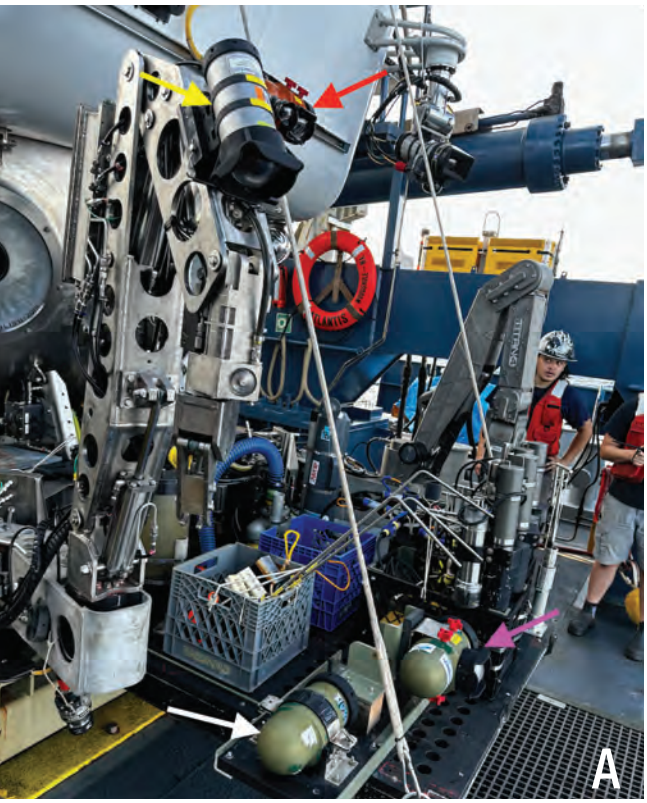

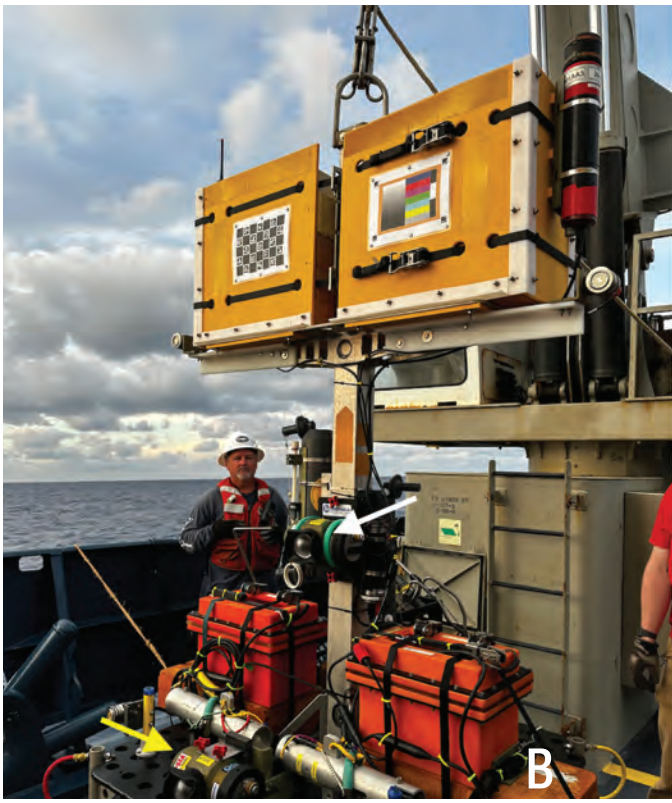

D. FORNARI, WHOI

Figure 5: MISO GoPro deep-sea camera systems on *Alvin* (A), a MISO/NDSF imaging lander (B), and ROV *Jason* (C). (A) shows four MISO GoPro cameras in various mounting positions. Red arrow shows Digi SeaCam with a HERO11™ camera module shooting 27MP still images every 5 sec for the duration of the dive's ~8-10 hrs. total operational time – deck to deck. Yellow arrow points to a MISO-OIS Super SeaCam camera with a HERO4™ camera shooting 4K video at 24 fps for the entire dive duration. White arrow shows a Digi SeaCam with a HERO11™ camera module shooting 5.3K cinematic video at 30 fps shooting vertically down from the front of *Alvin*'s sample basket. Lighting for this camera is provided by three DeepSea LED SeaLite (~9,000 lumens each) lights positioned behind and across from the camera mount position. Purple arrow shows a HERO11™ camera module shooting 5.3K cinematic video at 30 fps oriented to capture the terrain from a low, forward position as the submersible traverses the seafloor. Lighting for all forward-pointing cameras on *Alvin* is provided by 8-10 DeepSea LED lights. (B) shows the MISO/NDSF imaging lander as configured on an expedition in February 2024 (AT50-21) to the East Pacific Rise near 9° 50'N. Yellow arrow points to a MISO GoPro™ Digi SeaCam housing with a HERO11 module shooting 5.3K cinematic video at 30 fps, capturing vehicle operations. White arrow points to a MISO GoPro™ Digi SeaCam housing with a HERO11™ module shooting 27MP still images every 5 sec. Power for the lighting system consists of two 24 VDC DeepSea SeaBattery® power modules (orange housings) each with ~40 amp-hour capacity coupled to MISO deep-sea switches (silver cylinders above yellow arrow) that controls four DeepSea LED lights. Each switch is activated by *Alvin*'s manipulator when it moves a slide fixture with a magnetic reed switch. (C) shows the front of ROV *Jason* with two MISO-OIS Super SeaCam GoPro cameras mounted on the port manipulator (blue arrow) and a MISO Digi SeaCam GoPro camera for 27MP still imaging on the upper port light-bar of the vehicle (green arrow).

the best still images (27MP) of the work area in front of *Alvin* at sites in the Gulf of Mexico, Blake Outer Ridge, East Pacific Rise 9° 50'N, and Guaymas Basin, Gulf of California expeditions (AT50-04, AT50-05, AT50-06, and AT50-07, AT50-20, AT50-21, AT50-22), as well as 5.3K cinematic video imagery in various forward and down-looking orientations on *Alvin*'s front basket (Figure 5). It is important to note that these cameras require no tasking from observers or pilots during dives; they are set to record 27MP images every 5 sec, or continuous 5.3K cinematic video at 30 fps, and use *Alvin*'s LED lighting from DeepSea for illumination. The cameras have also been used to provide exceptional video and still imagery of *Alvin* and ROV *Jason* working at the seafloor study sites using the MISO GoPro™ camera systems on deep-sea landers positioned by the submersibles at several study areas (Figure 5).

During 2023-2024, DeepSea produced ten additional Digi SeaCam housings in an upgrade effort funded by NSF and DeepSea so that the MISO Facility can continue to support NSF-funded oceanographic research and provide deep-sea cameras to other deep submergence facility operators, both in the US and internationally (Figure 4).

MISO GoPro™ CAMERA SYSTEM COMPONENTS

DeepSea Power & Light – Super SeaCam® Corrector Optics

The underwater optical design used in the MISO GoPro deep-sea camera systems has a long history at DeepSea. Its development started in the late 1990s in an effort to improve the underwater imaging performance of an analog zoom camera based on Sony block camera modules from that time. Up to that point, camera optics in DeepSea products, such as those found in the Multi SeaCam 1000, SeaCam 1001, and SeaCam 3400 (all from the early 1990s), either relied on simple flat ports or used dome ports with correctors based on off-the-shelf diopter lenses sometimes paired with wide-angle adapters (Figures 6-7).

Compared to flat ports, dome ports offer significant advantages to an underwater camera designed to operate at the high hydrostatic pressures of deep-sea environments. This is due to the geometry of a dome, which provides more uniform stresses throughout the material under compression. Compression favours materials like glass and sapphire, which have a compressive strength many orders of magnitude higher than their tensile strength. In contrast, flat ports, by their nature, support high tensile stress on the inside surface due to the bending moment imparted on the port by the external pressure and the housing (Figure 6). Additionally, a flat port will introduce spherical distortion, chromatic aberration, and reduce the field of view of the lens system by close to the ratio of the index of refraction from air to water [15]. Much of this can be avoided with a dome port optical system. However, dome ports, too, pose some unique imaging challenges.

When looking through a dome underwater, a camera is presented with a virtual image where the entire field of view is pulled close to the camera. The virtual image is created by the negative meniscus lens formed by the refractive differences in air and water on either side of the dome port. Parallel rays entering the

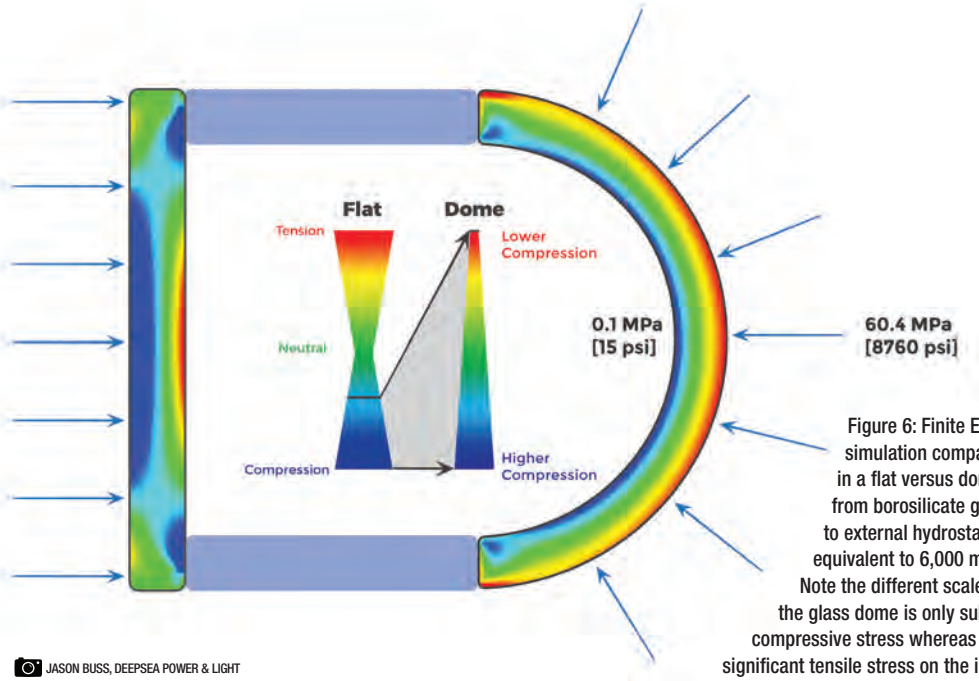

JASON BUSS, DEEPSEA POWER & LIGHT

Figure 6: Finite Element Analysis simulation comparing the stress in a flat versus dome port made from borosilicate glass subject to external hydrostatic pressure equivalent to 6,000 m in seawater. Note the different scales where the glass dome is only subjected to compressive stress whereas the flat port has significant tensile stress on the inside surface.

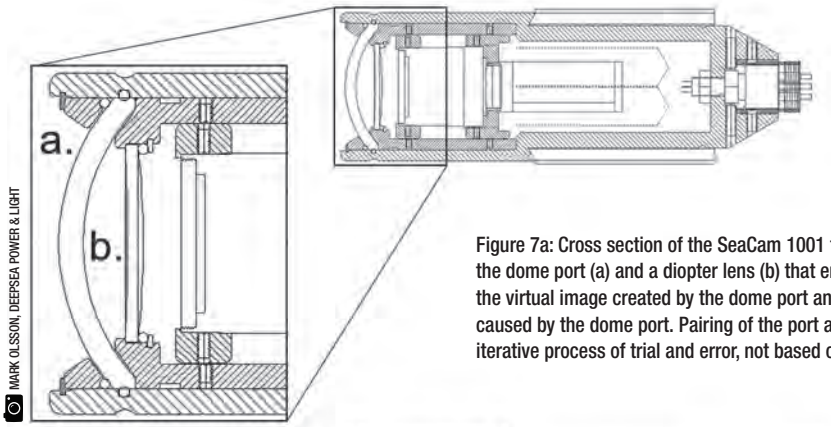

MARK OLSSON, DEEPSEA POWER & LIGHT

Figure 7a: Cross section of the SeaCam 1001 from the early 1990s showing the dome port (a) and a diopter lens (b) that enabled the camera to focus on the virtual image created by the dome port and flattened the field curvature caused by the dome port. Pairing of the port and corrector lens was an iterative process of trial and error, not based on simulation or modelling.

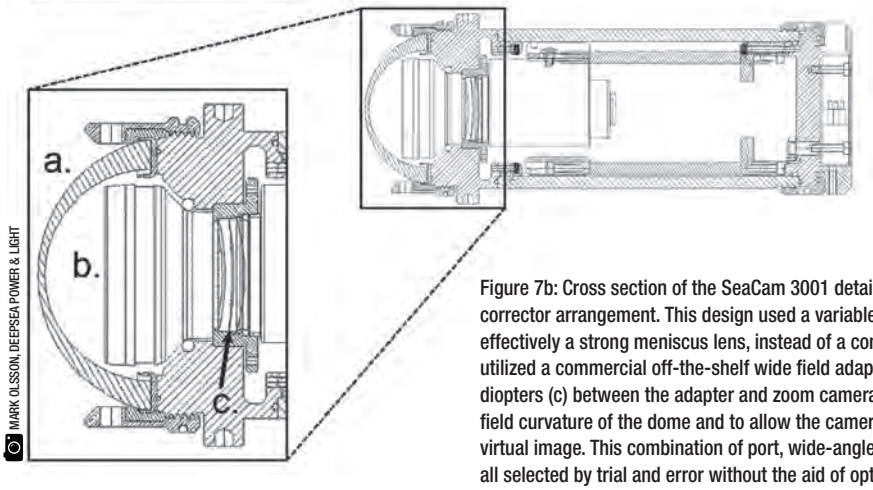

MARK OLSSON, DEEPSEA POWER & LIGHT

Figure 7b: Cross section of the SeaCam 3001 detailing the dome port and corrector arrangement. This design used a variable thickness dome (a), effectively a strong meniscus lens, instead of a constant thickness dome. It utilized a commercial off-the-shelf wide field adapter (b) but with a pair of diopters (c) between the adapter and zoom camera lens to correct for the field curvature of the dome and to allow the camera to focus on the close-in virtual image. This combination of port, wide-angle adapter, and diopters were all selected by trial and error without the aid of optical simulation tools.

dome appear to converge from a point much closer than infinity [16]. The consequence is that an object normally in focus at 2 m, 5 m, or 100 m will appear to be at a distance of ~4 times the radius of the dome relative to the dome's centre of curvature [17]. This can be well inside the minimum focus distance of many lenses designed for use in air, especially so with long telephoto zoom lenses, making it impossible for the camera to focus on the virtual image. The virtual image appears at approximately four times the dome radius if an infinitesimally thin dome is assumed. However, in practice for a dome with realistic thicknesses suitable for withstanding hydrostatic pressures found in the deep sea, this limit is brought in closer than 4 radii. (For a detailed derivation of the calculate of the virtual image distance for underwater domes, see [17].)

Diopters and other close-up lens adapters used in macro-photography work like a magnifying glass, allowing the camera to focus on this virtual image, effectively making the camera near-sighted [15a,b]. By matching the strength of the diopter to the distance of the negative dome-lens of the virtual image from the dome centre, infinity focus can be pushed back out. This is why dome port camera housing manufacturers such as Ikelite recommend a 4+ diopter when paired with a 6"-diameter dome port. The optical magnification of the diopter is close to the inverse of the virtual image location from the centre of curvature of the dome (in metres).

Wide-angle adapters, or focal reducers, shorten the focal length of the lens (a smaller focal length yields a wider field of view), which helps in two main ways:

1. Since the focal length is smaller but the aperture remains the same, the effective focal ratio, or F-number, also decreases. A smaller F-number means the optics gather more light and operate better in lower illumination conditions, which is a universal system design challenge at hadal depths.
2. Wide-angle adapters reduce the spatial resolution of the optics, which can hide chromatic aberration and distortion introduced by the dome port and diopter, effectively compressing them below the resolving power of the imaging system. The apparent size of the imaging artifacts become smaller and harder to resolve in the final image.

Some early DeepSea cameras successfully employed diopters and wide-angle adapters to correct the dome virtual image problem. Using a simple diopter and focal reducer in this way works sufficiently for large-radius optical dome ports where the ratio of the dome radius to the sensor diagonal or film frame diagonal is around 10:1. Small dome-to-sensor ratios are harder to design for when developing an optical dome system for high pressure, deep-ocean applications. For these uses, thicker glass walls are needed to withstand the external hydrostatic pressures, and the engineering and manufacturing difficulties increase exponentially with the size of the dome port. Diffraction inside the thicker dome also plays a more significant role in the overall complexity of the optical design, as does proper optical alignment [15a,b] and stray light mitigation. In practice, diopters also introduce chromatic aberration and other forms of optical distortion that reduce image quality, especially at the extreme angles of the field of view.

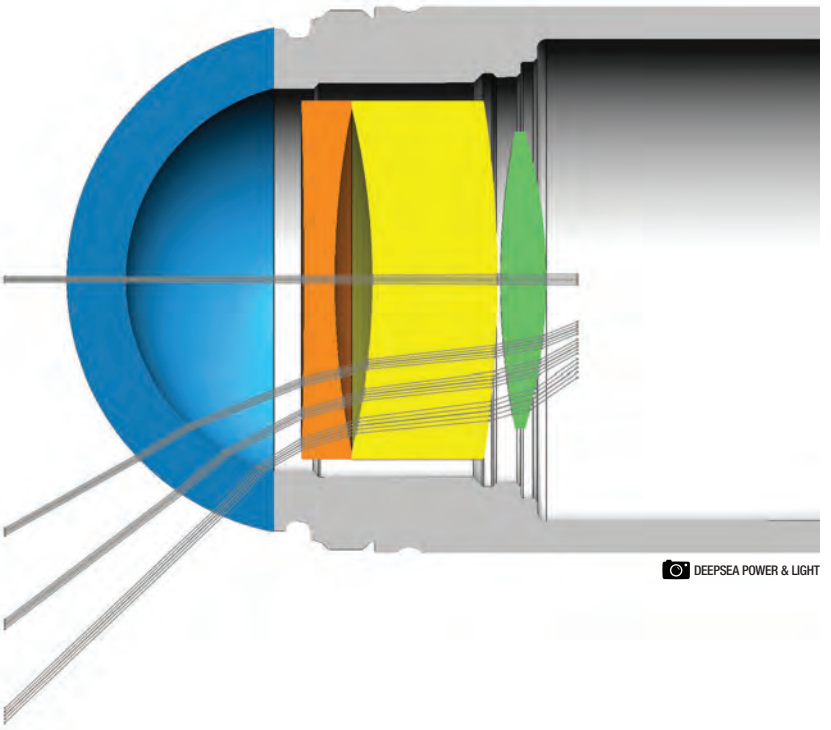

DEEPSEA POWER & LIGHT

Figure 8: Ray trace diagram showing the refracted light rays through a dome port and the custom lens elements of an example three element corrector design. The rays entering the dome are wider than the rays entering the camera objective that would be located behind the green lens element showing how this grouping provides field widening in addition to correcting for the field curvature and virtual image produced by the dome.

The dome port also introduces distortion into the focal plane on the sensor or film area, often making it difficult to get proper focus across the entire field of view at large apertures. Instead of the sharp focus area of the projected image being uniform across the image area, it is spherical. This increases in severity as the dome radius shrinks, making it an even harder problem on smaller high-pressure domes. Testing and iteration with dome dimensions, diopter strength, and different focal reducers would produce a viable solution in many cases, but not all. Nor could it adequately address the various chromatic and geometric distortion and optical aberrations that degrade imaging performance. DeepSea engineers decided to take a more scientific approach to solving the problem. Designing a custom optical corrector was the key that would enable sharp, fast, and low-distortion imaging across a wide range of focal lengths (Figure 8).

DeepSea engineers compiled data about wide-range varifocal lenses used in the block cameras of interest from published patents [18] and from lab measurements in order to build a digital model of the optical system – a paraxial approximation that preserves the first order relationship between rays entering and exiting a lens. After setting up these models at different focal lengths and different focus positions, the models could be used to simulate the performance of different corrector and dome port designs. Optical design software Zemax OpticStudio served as the design simulation and optimization tool for this task (https://www.ansys.com/products/optics/ansys-zemax-opticstudio). A skilled optical designer can use Zemax to find promising local minima throughout the possible configuration space to further develop and optimize. This search is constrained by limiting parameters like the number of optical

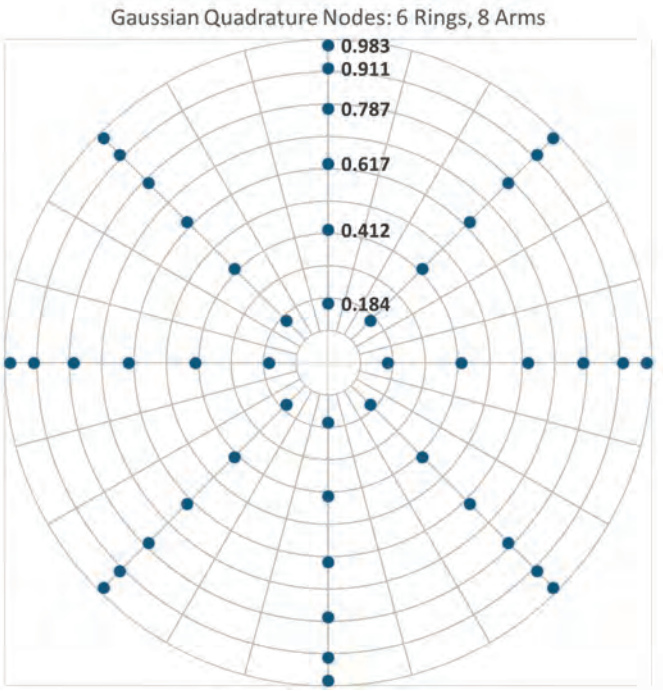

DEEPSEA POWER & LIGHT

Figure 9 (left): Polar plot showing the distribution of node locations used by the Zemax merit function to evaluate the wavefront error of a simulated optical corrector during optimization. Rays of light at different wavelengths at these nodes are launched through the optics and the resulting projections produce a spot diagram. The Zemax merit function yields a weighted sum of the RMS radii of these projected spots as feedback to the optimizer to minimize the spot sizes across all of the nodes.

Figure 10 (below): Example spot diagram from Zemax showing the spread and shift of three different wavelengths of light launched from simulated point sources into the dome and corrector optics. Each grouping of red, green, and blue points represents the projected image on the camera sensor from a point source at a particular distance from the camera. The shape, size, and distribution of these groupings will show the effects of different kinds of distortion such as astigmatism, coma, chromatic aberration, lateral colour shift, and spherical aberration. In this case the RMS radius of each grouping is less than 3µm, smaller than the pixel size of the imager.

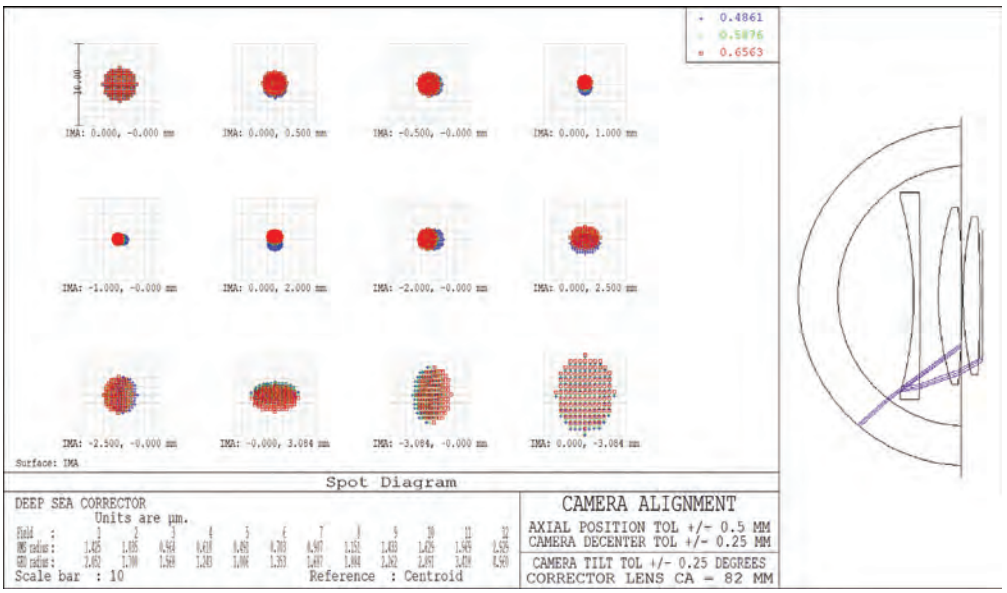

DEEPSEA POWER & LIGHT

elements, lens sizes, glass types, and the optical bandwidth of the target design.

For this design, the merit function calculated the error between the target performance and a specific design candidate by simulating an array of points of light in the image space and tracing the path they take through the optics to the exit pupil of the candidate lens design. Zemax uses the Gaussian Quadrature numerical method [19] to integrate the error between the spots formed by these rays and the ideal spot sizes. In Figure 9, an array of nodes at the intersection of six rings and eight arms defined the location of the simulated point sources (Figures 9-10).

For the design of the Super SeaCam corrector used in the Digi SeaCam, the dome size and dimensions were fixed based on the mechanical constraints of designing a dome port to withstand high external hydrostatic pressure. The paraxial approximations of the zoom camera lens at different focal lengths and object distances were all used in parallel to optimize the corrector lens prescription. The role of the optics designer is to use knowledge of lens design and experience to set a starting point for the optimizer to build from. Here a two-element corrector was set as the starting condition. The Zemax optimizer was able to vary the diameter and curvature of the lens surfaces, the types of glass, the air gaps between elements, and the thickness of the lenses and through thousands of iterations arrived at an optimal solution. The result of this effort was a three-element high pressure corrected dome port optic (two lens elements plus the dome), which:

- provided precise magnification matched to the virtual image formed by the dome;
- reduced the focal length to improve sensitivity and widen the field of view;
- flattened the focal plane, in order to produce a sharp image across the imaging area;
- corrected geometric and chromatic aberration introduced by the dome;
- compressed the field of view, making it easier to keep foreground and background objects in focus at the same time; and
- worked across a wide range of imaging lens configurations and focal lengths.

In essence, this solution had all the benefits of the diopter-plus-focal-reducer solution while reducing the optical aberrations created by the dome instead of amplifying them. The result was a corrector that greatly improved imaging performance across use cases, including in challenging deep-ocean environments.

The DeepSea optical corrector was first introduced in the Super SeaCam in 2000. Soon after, DeepSea worked with the WHOI MISO Facility to adapt the same optical solution to work with a 3.3MP Nikon Coolpix 995 (https://en.wikipedia.org/wiki/Nikon_Coolpix_995) still image camera, resulting in the unusual side-port configured 6,000 m rated Digi SeaCam (https://www2.whoi.edu/site/miso/miso-instrumentation/deep-sea-cameras-and-strobes) in 2002. As previously noted, the Digi SeaCam was a key component of the MISO *TowCam* systems and used for numerous research expeditions providing data for dozens of research publications and student theses (see Figure 1 and Table 1).

DeepSea continues to use this versatile optical corrector solution in the modern Optim® SeaCam 4K subsea camera family, which, with a maximum 11,000 m operating depth, has unrestricted access to all corners of the ocean.

Back-Bone – GoPro HERO4™ and HERO11™ Cameras – Special 5.4 mm Lens Integration

As noted above, in 2014, the GoPro HERO4 Black™ camera was initially chosen as a candidate for upgrading MISO deep-sea imaging capabilities due to the camera's small form factor, ease of operation, and high-end specifications.

However, integrating the camera into the DeepSea housing required thoughtful

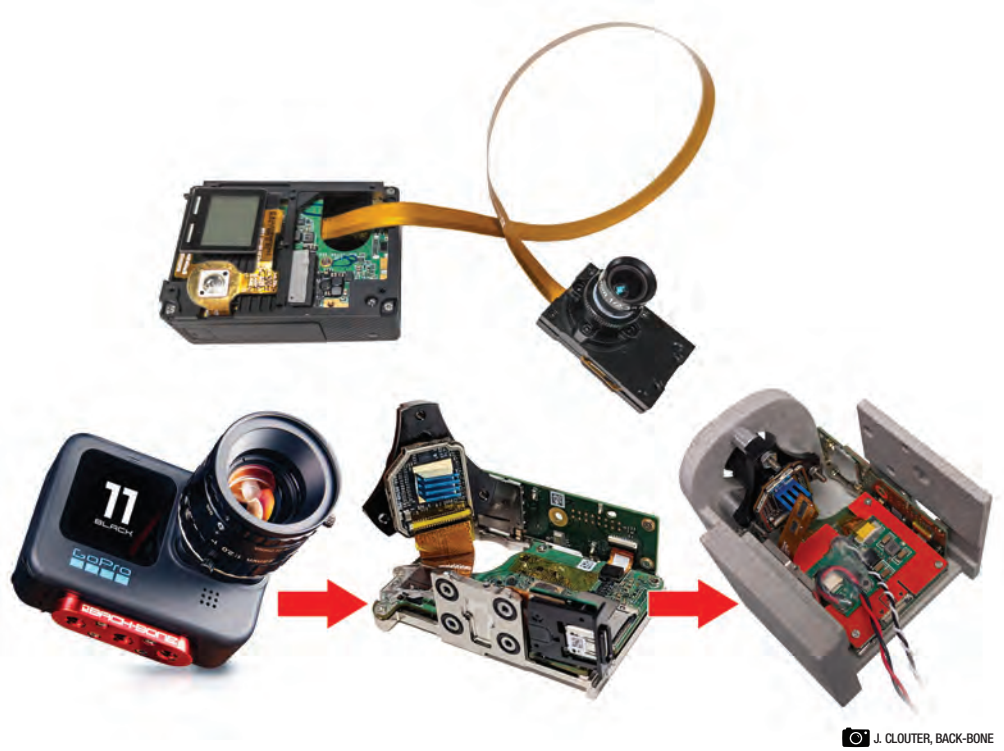

J. CLOUTER, BACK-BONE

Figure 11: (Top) Back-Bone HERO4™ lens relocation modification system. (Bottom) Back-Bone HERO11™ reconfiguration used in the DeepSea Optim 11 km housing, which was configured for the *Alvin* submersible as a GoPro-based 27MP still camera for routine operations down to the submersibles' 6,500 m rated operational depth (note that *Alvin* safety protocols as prescribed by the US Navy requires a pressure certification procedure that includes nine 10-minute cycles to ~1.5x the vehicle-rated operational depth and a final tenth cycle where that pressure is held for 1 hour). The Back-Bone and EPO-OIS collaboration to integrate the HERO11™ module into the Optim SeaCam 11 km-rated housing resulted in a routinely operable, very high-resolution camera for enhanced science capabilities to *Alvin*'s maximum operating depth of 6,500 m.

engineering changes to the camera form-factor. Though the original camera is physically small, it features an offset lens, making it difficult to centre in the optimal position behind the existing DeepSea corrector optics. In fact, the offset lens makes it impossible to mount in the existing DeepSea housings rated for 6,000 m. In 2014, the only available housing other than the Digi SeaCam housing with this corrector was the Super SeaCam, which had a max depth rating of 6,000 m. The 11,000 m depth rating would not be realized until the newer DeepSea Optim SeaCam housing was released in 2019. Furthermore, the wide-angle fisheye lens built into the original camera is not well suited for combination with the DeepSea optical system; when paired with the corrector optics, its wide-angle field of view resulted in increased chromatic aberration towards the edges, and interior views of the dome were visible.

By 2014, Back-Bone had already developed interchangeable lens modifications for both the GoPro HERO3 and HERO4 cameras. The MISO project coincided with an internal Back-Bone project named "Modulus," which expanded on these modifications. As part of that project, the HERO4's 1/2.3" CMOS sensor was detached from the camera body and extended up to 30 cm via a custom-designed flex ribbon. The CMOS sensor was housed in its own aluminum shell complete with lens mounts for M12, CS-Mount, and C-Mount lens types (Figure 11). That configuration allowed the camera body to fit lengthwise into even the smallest pressure vessels while the CMOS sensor and lens were

precisely positioned and centred behind the previously developed corrector optics.

With the form factor and lens mount issues addressed, the optics needed to be selected. The M12 (S-mount) lens type was chosen given the format's extremely small size and high resolution. A rectilinear 1/2.3" 5.4 mm lens provided excellent results in a variety of tests and provides an image with none of the "fisheye" distortion that is often associated with GoPro™ cameras. Its fixed focus design has a depth of field ranging from 0.5 m to infinity as well as having an optimal field of view while not capturing interior views of the dome.

In 2022, Back-Bone's standard H11PRO modified HERO11™ camera paired with the same 5.4 mm lens began service in DeepSea camera housings used by the MISO Facility (Figures 3-5 and 11-12). The new, larger 1/1.9" image sensor features significant image quality and resolution improvements over the HERO4™ but still features an offset lens, so the challenge of mounting the camera inside the newer 11,000 m rated housings needed to be addressed. Given the time window needed for a rapid deployment, the development of a new CMOS flex ribbon extension was not viable. Instead, a stripped-down version of the camera was developed with a dedicated M12 lens mount attached. In collaboration with EPO, this version of the camera was developed so that the CMOS and lens are securely mounted at a 90-degree angle to the main camera body. That configuration allows the assembly to fit into the DeepSea Optim SeaCam housing and slide forward into the proper position behind the dome's corrector optics (Figures 12-13).

EXAMPLES OF MISO GoPro™ CAMERA SYSTEMS IMAGERY FROM NATIONAL SCIENCE FOUNDATION FUNDED EXPEDITIONS

Scientific expeditions utilizing the MISO GoPro™ camera systems have captured fundamental seafloor processes at mesophotic reefs, spreading centres, seamounts, seeps, canyons, and hydrothermal vents (Figures 14-25). Access to high-resolution, infinite-focus imagery at these sites has been transformative for performing modern analyses on 1) seafloor habitat classification and mapping, 2) counting individuals of different fauna, 3) non-invasive computation of fluid fluxes, and 4) creating 3D renderings of complex structures. This section provides some exemplar imagery from NSF-funded expeditions from 2022 through 2024, using 2nd and 3rd generation MISO GoPro cameras in both the DeepSea Digi SeaCam and Super SeaCam housings.

DISCUSSION AND CONCLUSIONS

High resolution still and video imagery produced by the MISO Facility deep-sea cameras, and especially the new MISO GoPro cameras, have contributed to dozens of peer-reviewed scientific publications as well as numerous educational and outreach activities that highlight multi-disciplinary oceanographic research to the public and stimulate students at all levels, from K-12 to undergraduate and graduate students (see references listed in Supplementary Material). Imagery from MISO camera systems have also been used in artistic projects as a visual portal for the lay public to the largely inaccessible environments of the deep ocean. Images and

D. FORNARI, WHOI

Figure 12: 11 km-rated DeepSea Optim SeaCam camera housing for *Alvin*'s GoPro HERO11™ still and video camera system resulting from the collaboration between DeepSea, EPO-OIS, Back-Bone, and the WHOI-MISO Facility. The three-element high pressure corrected dome port optic (two lens elements plus the dome) is the same design as the one used in the DeepSea Digi SeaCam and Super SeaCam housings (see Figures 3-5).

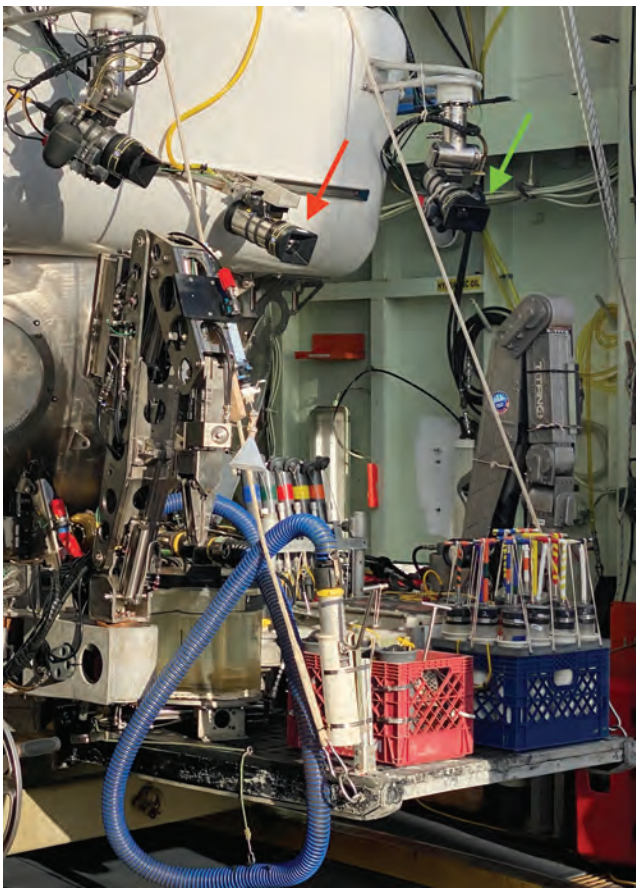

DR. TIM SHANK, WHOI

Figure 13: *Alvin*'s imaging and sampling equipment configured for deep (~5,000 m) dives in the Aleutian Trench in June 2024. Red arrow shows DeepSea Optim 11 km housing with integrated HERO11 imaging module resulting from collaboration between DeepSea, EPO-OIS, Back-Bone, and WHOI-MISO Facility used on *Alvin* for 27MP still imaging at 5 second intervals for deep dives to 6,500 m depth. Camera is mounted above pilot's viewport next to a DeepSea HD Multi Seacam HD video camera (centre). Camera at upper right and left on pan-and-tilt units are two DeepSea 4K Optim SeaCam video cameras (green arrow) used for 4K, user-controlled, video imagery acquisition as part of the standard data package on every dive.

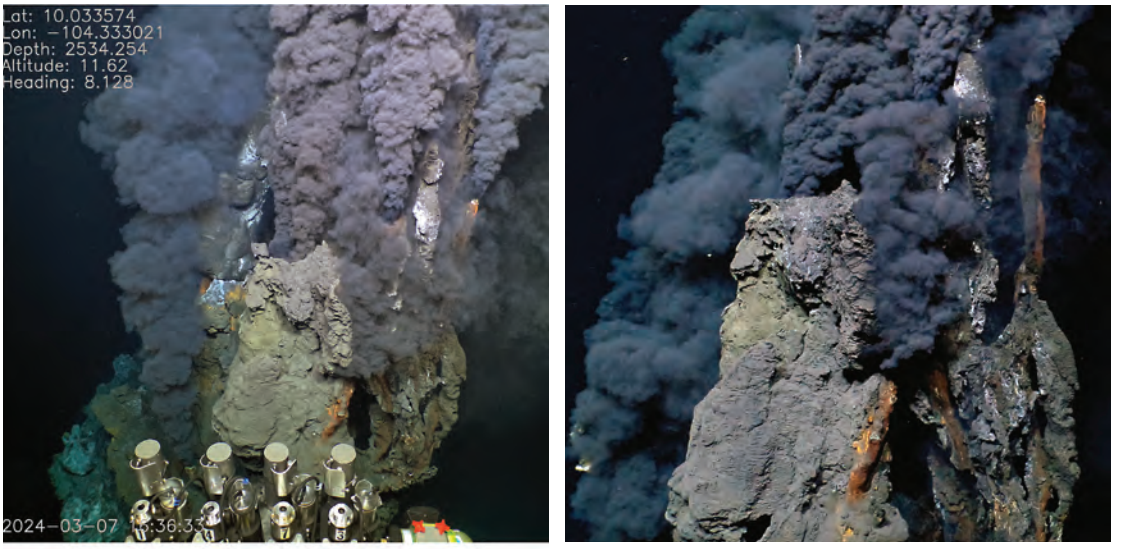

Figure 14: (Left) 27MP image of newly discovered hydrothermal vent at 2,534 m depth on the axis of the East Pacific Rise near 10°N acquired with the 3rd generation MISO Digi SeaCam system using a GoPro HERO11™ camera on *Alvin*'s "brow" (above pilot's viewport); notations in the image are metadata from *Alvin*'s data system synchronized (in UTC) to the image "creation" date/time. (Right) Digital screengrab of the 5.3K cinematic video at the same vent acquired simultaneously at 30 fps, by the basket-mounted, forward-looking MISO Digi SeaCam system on *Alvin* during Dive 5245 in March 2024.

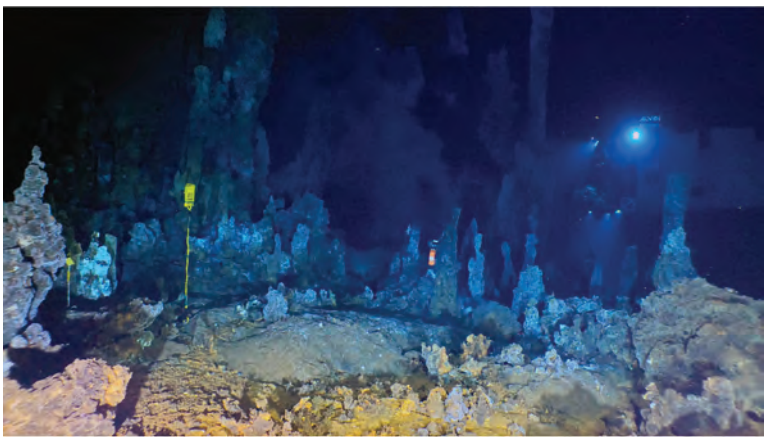

Figure 15: (Top) Digital screengrab of the 5.3K cinematic video acquired at 30 fps by the lander-mounted, forward-looking 3rd generation MISO Digi SeaCam system deployed during *Alvin* Dive 5249 in March 2024 at the YBW-Sentry hydrothermal field at 2,540 m depth, near 9° 54'N [20]. (Bottom) 27MP image of the MISO-NDSF imaging lander with the 3rd generation MISO Digi SeaCam system using a GoPro HERO11™ camera on *Alvin's* "brow" (above pilot's viewport).

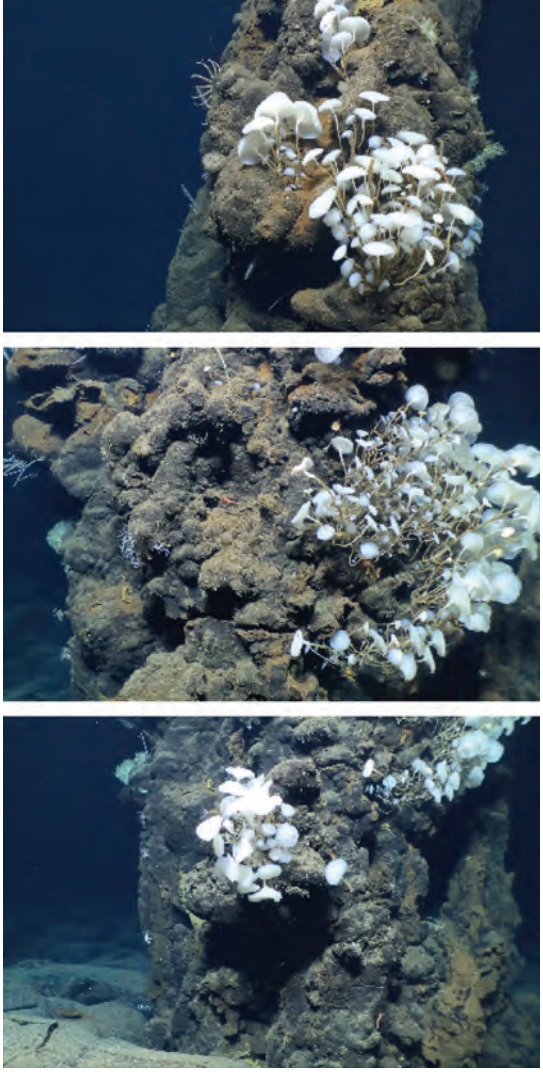

V. PRESTON AND MCDERMOTT, FORNARI, BARREYRE, PARNELL-TURNER, AT50-21, WHOI-NDSF, NSF, MISO FACILITY

Figure 16: (Left) Sequence of digital screengrabs of an inactive hydrothermal vent colonized by a variety of sessile and mobile fauna, surrounded by lava likely erupted in ~2005-2006 at the East Pacific Rise near 9° 47'N west of the axis. Imagery is from 4K video acquired at 24 fps using a GoPro HERO4™ camera module in the 2nd generation MISO-OIS Super SeaCam housing. The camera was mounted on *Alvin*'s starboard arm during Dive 5236 in March 2024. (Right) The orthomosaic was assembled from a 3D reconstruction of 531 images extracted from the 4K video. The spire was imaged by moving the submersible up and down the structure in a scanning pattern. Agisoft Metashape (https://www.agisoft.com/) was used to compute the 3D reconstruction and orthomosaic. No other post-processing has been performed on the imagery.

MCDERMOTT, FORNARI, BARREYRE, PARNELL-TURNER, AT50-21, WHOI-NDSF, NSF, MISO FACILITY, ©WHOI, 2024

Figure 17: Framegrabs of 5.3K video from 3rd generation MISO GoPro camera system using a HERO11™ camera module and special 5.4 mm non-distortion lens in a DeepSea Digi SeaCam housing mounted on *Alvin*'s basket. The feature is a lava pillar that serves as the host for a large anemone and smaller brisgnid sea stars and a small sponge near the base of the anemone. The left image was acquired when the pilot drove close to the top of the lava pillar, filling the video frame with the anemone during *Alvin* Dive 5247 in March 2024.

Figure 18: 27MP image from a 3rd generation MISO GoPro camera system using a HERO11™ camera module and special 5.4 mm non-distortion lens, shooting at 5 s intervals, in a DeepSea Digi SeaCam housing mounted on the MISO-NDSF imaging lander near the Bio9 hydrothermal vent at 2,510 m depth on the axis of the East Pacific Rise near 9° 50'N. The instrument inserted in the hydrothermal vent is a MISO-OIS designed high-temperature logger measuring exit-fluid temperature at the vent every 10 min for a ~two-year period [21].

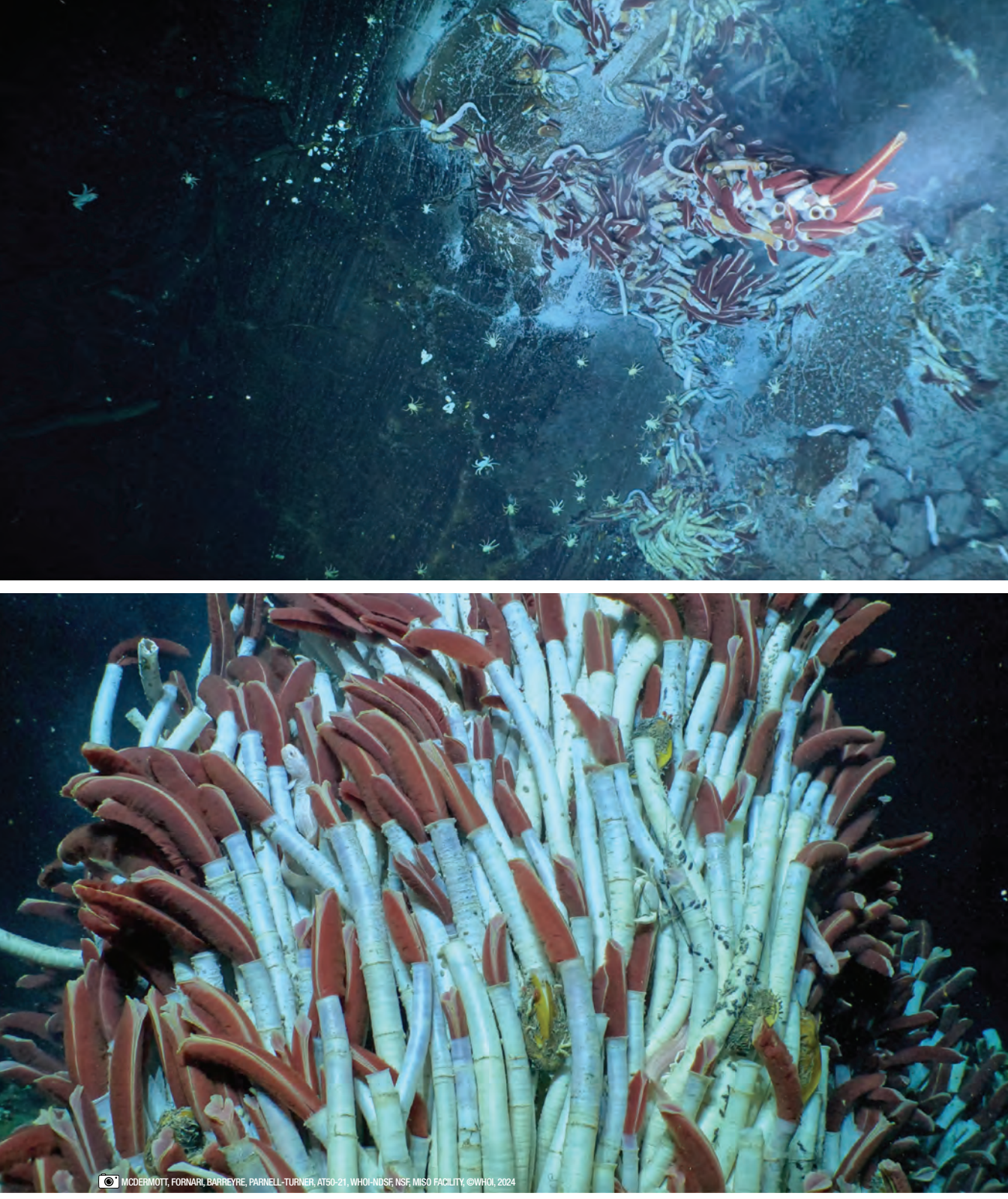

Figure 19: Framegrabs of 5.3K video from 3rd generation MISO GoPro™ camera system using a HERO11™ camera module and special 5.4 mm non-distortion lens in a DeepSea Digi SeaCam housing mounted on *Alvin*'s basket oriented looking down (top image) and looking forward (bottom image). Giant "Riftia" tubeworms at Biovent hydrothermal vent near 9° 51'N along the axis of the East Pacific Rise near 9° 51'N. Imagery was acquired during *Alvin* Dives 5244 (top) and 5243 (bottom).

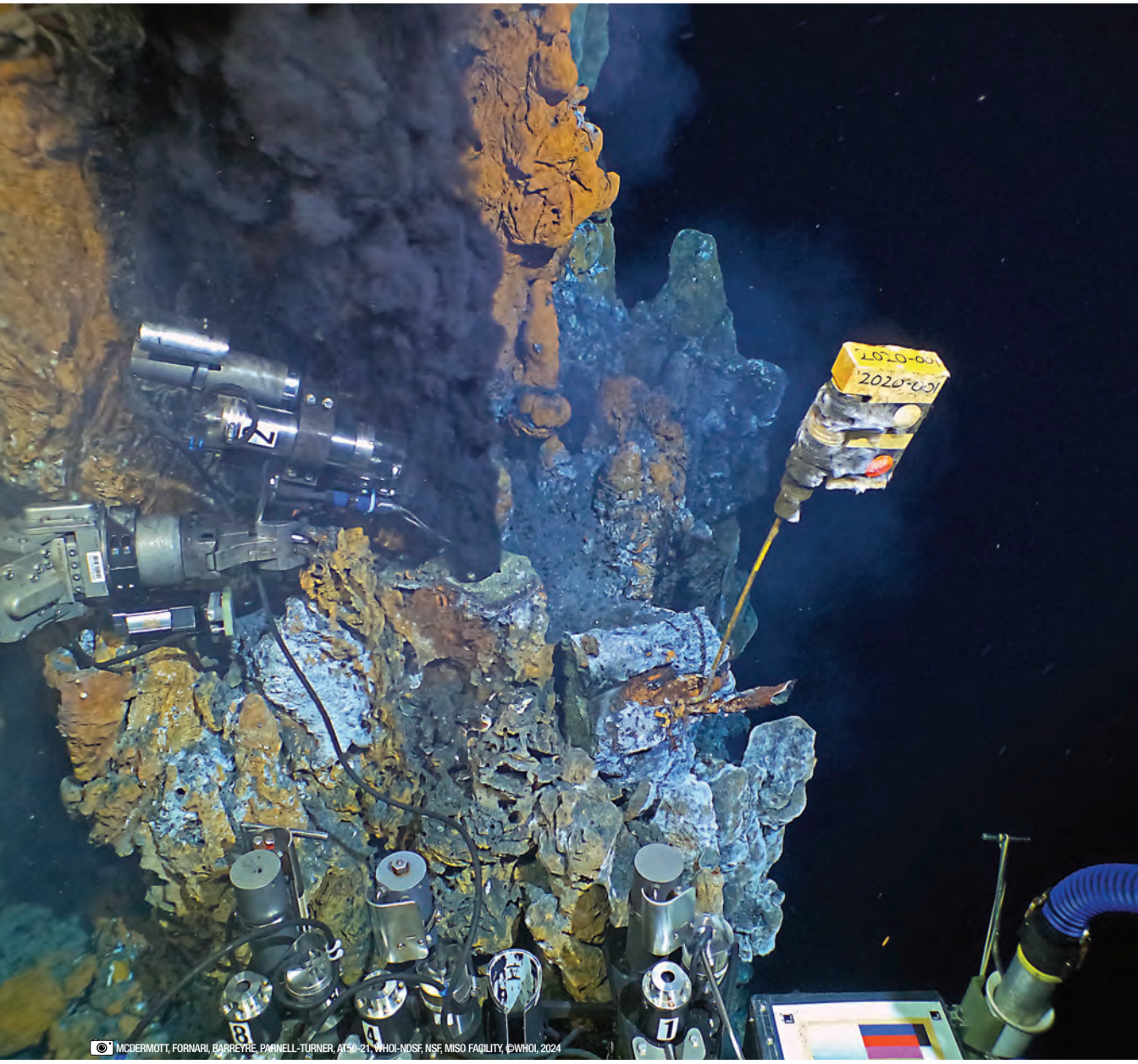

Figure 20: 27MP image of hydrothermal fluid sampling at "Nick's" vent during Dive 5235 at the YBW-Sentry hydrothermal vent ~700 m east of the axis of the East Pacific Rise near 9° 54'N in February 2024. Image was shot using a 3rd generation MISO Digi SeaCam system using a GoPro HERO11™ camera on *Alvin*'s "brow" (above pilot's viewport). Instrument to the right of the vent orifice is a EPO-MISO high-temperature vent fluid logger [21] that was imbedded in the chimney top that was broken off the structure to allow the fluid sample to be collected.

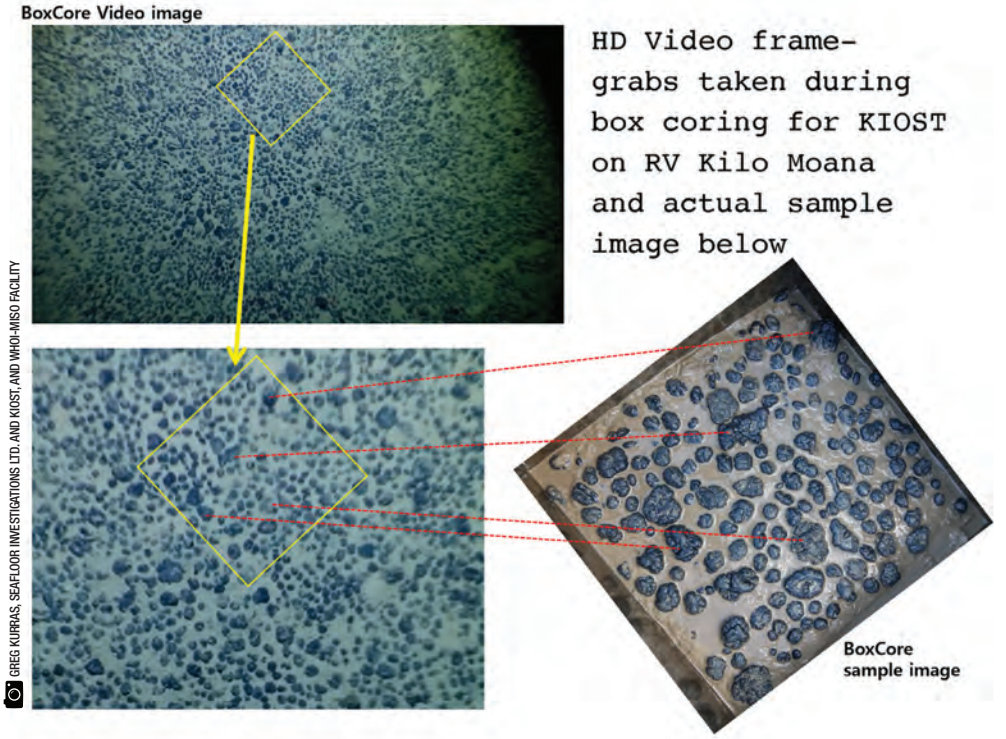

Figure 21: (Top) Box corer rigged with a 1st generation MISO GoPro camera used to take seafloor samples at ~5,000 m depth from the Clipperton-Clarion Mn-nodule field near 10°N. (Bottom) Framegrabs of 1080P video shot using a HERO4™ camera during bottom approach (~5 m altitude) and landing (~2 m altitude), and photograph (right-bottom) of the top surface of the box core on recovery and correlation of nodules shown in the imagery with actual recovered samples.

Figure 22: Sequence of framegrabs of 5.3K video from 3rd generation MISO GoPro™ camera system using a HERO11™ camera module and special 5.4 mm non-distortion lens in a DeepSea Digi SeaCam housing mounted on *Alvin*'s basket oriented looking forward. Superb depth of field is apparent in the middle image especially, given the close, in focus subject matter of the vent mussels very close (~<0.25 m) to the camera dome and far field focus of the fish and white cylindrical TCM-3 current meter instrument in mid-left centre of image. Imagery from a seafloor seep site in the Gulf of Mexico acquired during expedition AT50-04 (Courtesy of Prof. Craig Young, Institute of Marine Biology, University of Oregon).

Figure 23: Lava pillars supporting a rampart formed during the 2005-2006 volcanic eruption at the East Pacific Rise near 9° 50'N. Image is a framegrab of 5.3K video from a 3rd generation MISO GoPro™ camera system using a HERO11™ camera module and special 5.4 mm non-distortion lens in a DeepSea Digi SeaCam housing mounted on *Alvin*'s basket oriented looking forward during Dive 5236. Image width is ~4 m.

Figure 24: Framegrab of a Dumbo octopus (likely *Cirrothauma cf. murrayi*) at ~2,530 m depth on the axis of the East Pacific Rise from acquisition of 5.3K video in a 3rd generation MISO GoPro™ camera system using a HERO11™ camera module and special 5.4 mm non-distortion lens in a DeepSea Digi SeaCam housing mounted on *Alvin*'s basket oriented looking forward. Image width is ~1 m.

Figure 25: *Alvin* being recovered by RV *Atlantis*, from a dive in March 2024 during expedition AT50-21. Four MISO GoPro camera systems are mounted on the submersible, in addition to two DeepSea 4K Optim cameras on port and starboard pan and tilt systems (see also Figure 13).

video from MISO cameras have contributed to academic websites, have been used to support research documented in peer-reviewed publications, are used to highlight technology improvements in industry/technical publications, and are being used for several high-profile filming projects. These latter projects include: 1) a 3D IMAX film (tentative title: *Born in the Abyss*, based on research by C. Young (Institute of Marine Biology, University of Oregon) being produced with NSF funding by Stephen and Alex Low (NSF OCE-1851313, plus supplement OCE-2234492) *Collaborative research: dispersal depth and the transport of larvae around a biogeographic barrier*, and

OCE-2215612 *Using media and technology to advance public awareness of research on microscopic larvae in the deep ocean*; 2) a BBC production series *Planet Earth III* where filming of *Alvin* supporting research at mid-ocean ridge hydrothermal vents at the East Pacific Rise near 9° 50'N has been highlighted (aired in November 2023); and 3) a future BBC production, *Blue Planet III*, expected to air in 2026.

ACKNOWLEDGMENT

The authors wish to thank colleagues in the DeepSea and WHOI-MISO teams who have helped through the years to foster improvement in camera and instrumentation designs. The DeepSea authors would like to acknowledge their colleagues: Brian Braden, Hector Duran, Bruce McDermott, and Hooman Zarrabian for their extensive efforts in making these imaging systems possible and contributing to their ongoing success, as well as Amy Doria for her support throughout the creation of this article. DJF would like to acknowledge the following members of the WHOI-MISO team and research colleagues who have been instrumental to the success of the MISO Facility and the development of the deep-sea camera systems operated for the academic community: Bill Ryan, Adam Soule, Tim Shank, Marshall Swartz, Chris Lumping, Mark St. Pierre, Tim Smith, Don Collasius, Bruce Strickrott, Anthony Tarantino, Rick Sanger, Lane Abrams, Steve Liberatore, Rod Catanach, Andy Billings, Eric Hayden, Terry Hammar, Rhian Waller, Will Ridgeon, Jon Howland, Dana Yoerger, Hanu Singh, Greg Kurras, Allison Fundis, Sean Kelley, Matt Silvia, Justin Fuji, Nick Matthews, Ben Freiberg, Thibaut Barreyre, Jill McDermott, and Ross Parnell-Turner. In addition, James Holik, a facilities program manager recently retired from the National Science Foundation's Ocean Instrumentation Program, provided essential support for operation of the MISO Facility and development of new camera systems over the past 12 years, including the numerous MISO GoPro cameras now widely used in the US academic research community. This work has been supported by the following US National Science Foundation research grants to DJF at WHOI: OCE-1824508, OCE-1949485, and OCE-2313521.

REFERENCES

1. Edgerton, H.E. [1963]. *Underwater photography.* In: The sea, ideas, and observations on progress in the study of the seas. Vol. 3, edited by M.N. Hill, pp. 473-475, John Wiley & Sons, New York.
2. Ewing, M.A.; Vine, A.C.; and Worzel, J.L. [1946]. *Photography of the ocean bottom*. Journal of the Optical Society of America, 36, 307.
3. Hersey, J.B. (ed.) [1967]. *Deep-sea photography*. Baltimore: The Johns Hopkins University Press.
4. Karson, J.; Kelley, D.; Fornari, D.; Perfit, M.; and Shank, T. [2015]. *Discovering the deep: a photographic atlas of the seafloor and ocean crust*. Cambridge U. Press.
5. Heezen, B.C. and Hollister, C.D. [1971]. *The face of the deep*. New York: Oxford University Press.
6. Spiess, F.N. and Tyce, R.C. [1973]. *Marine Physical Laboratory Deep Tow Instrumentation System*. Ref. 73-4, Scripps Inst. Oceanogr., Lab Jolla, Calif.
7. Ballard, R.D. and Moore, J.G. [1977]. *Photographic atlas of the Mid-Atlantic Ridge Rift Valley*, 114 pp., Springer-Verlag, New York.
8. Grassle, J.F.; Berg, C.J.; Childress, J.J.; et al. [1979]. *Galápagos '79: initial findings of a deep-sea biological quest*. Oceanus, 22(2), 2-10.
9. Lonsdale, P. and Spiess, F.N. [1980]. *Deep-tow observations at the East Pacific Rise, 8˚45'N, and some interpretations*. Initial Rep. Deep Sea Drill. Proj., 54, 43.
10. Benthos Inc. [1984]. *Underwater photography, scientific and engineering applications*. New York: Van Nostrand Reinhold.

11. Ballard, R.D. [1985]. *The Titanic: lost and found – introduction*. Oceanus, 28, 4.
12. ARGO Rise Group [1988]. *Geological mapping of the East Pacific Rise axis (10°19'-11°53'N) using the ARGO and ANGUS image systems*. Can. Mineralogist, 26, 467-486.
13. Fornari, D.J. [2003]. *A new deep-sea towed digital camera and multi-rock coring system*. Eos, Trans. Am. Geophys. Union, 84, 69 & 73.
14. Fornari et al. [2019]. *Quiescent imaging article*. In Ocean News and Technology, August, www.oceannews.com.
15a. Menna, F.; Nocerino, E.; and Remondino, F. [2017a]. *Optical aberrations in underwater photogrammetry with flat and hemispherical dome ports*. In Videometrics, Range Imaging, and Applications XIV (Vol. 10332, pp. 28-41). SPIE.
15b. Menna, F.; Nocerino, E.; and Remondino, F. [2017b]. *Flat versus hemispherical dome ports in underwater photogrammetry*. The International Archives of the Photogrammetry, Remote Sensing and Spatial Information Sciences, 42, 481-487.
16. Menna, F.; Nocerino, E.; Fassi, F.; and Remondino, F. [2016]. *Geometric and optic characterization of a hemispherical dome port for underwater photogrammetry*. Sensors, 16(1), 48.
17. Knight, D. [2012]. *Dome port theory*. G3YNH. (https://g3ynh.info/photography/articles/dp_theory.html).
18. Kondo, T.; Kikuchi, A.; Kohashi, T.; Kato, F.; and Hirota, K. [1992]. *Digital color video camera with auto-focus, auto-exposure and auto-white balance, and an auto exposure system therefore which compensates for abnormal lighting* (U.S. Patent No. 5,093,716). U.S. Patent and Trade-mark Office. https://ppubs.uspto.gov/dirsearch-public/print/downloadPdf/5093716.
19. Forbes, G.W. [1988]. *Optical system assessment for design: numerical ray tracing in the Gaussian pupil*. JOSA A, 5(11), 1943-1956.
20. McDermott, J.M.; Parnell-turner, R.; Barreyre, T.; Herrera, S.; Downing, C.C.; Pittoors, N.C.; et al. [2022]. *Discovery of active off-axis hydrothermal vents at 9 ° 54 0 N East Pacific Rise*. Proceedings of the National Academy of Sciences of the United States of America, 119(31), 1-8. https://doi.org/10.1073/pnas.2205602119/-/DCSupplemental. Published.
21. Barreyre, T.; Parnell-Turner, R.; Wu, J.-N.; and Fornari, D. J. [2022]. *Tracking crustal permeability and hydrothermal response during seafloor eruptions at the East Pacific Rise, 9°50'N*. Geophysical Research Letters, 49, e2021GL095459. https://doi.org/10.1029/2021GL095459.

SUPPLEMENTARY MATERIAL

Peer-reviewed references using deep-sea photography and MISO camera and instrument systems.

ARGO Rise Group [1988]. *Geological mapping of the East Pacific Rise axis (1019'-1153'N) using the ARGO and ANGUS image systems*. Can. Mineralogist, 26, 467-486.

Ballard, R.D. and Moore, J.G. [1977]. *Photographic atlas of the Mid-Atlantic Ridge Rift Valley*. 114 pp., Springer-Verlag, New York.

Barreyre, T.; Parnell-Turner, R.; Wu, J.-N.; and Fornari, D. J. [2022]. *Tracking crustal permeability and hydrothermal response during seafloor eruptions at the East Pacific Rise, 9°50'N*. Geophysical Research Letters, 49, e2021GL095459. https://doi.org/10.1029/2021GL095459.

Cowen, J.; Fornari, D.J.; Shank, T.M. [n.d.]. *Rapid response to a volcanic eruption at the East Pacific Rise Crest near 9° 50'N*. Eos, Trans. American Geophys. Union.

Delaney, J.R.; Kelley, D.S.; Lilley, M.D.; et al. [1998]. *The quantum event of oceanic crustal accretion: impacts of diking at Mid-Ocean Ridges*. Science, 281, 222-230.

Edgerton, H.E. [1963]. *Underwater photography in the sea*. Ideas and Observations on Progress in the Study of the Seas, Vol. 3, edited by M.N. Hill, pp. 473-475, John Wiley & Sons, New York.

Edwards, M.H.; Smith, M.O.; and Fornari, D.J. [1992]. *CCD digital camera maps the East Pacific Rise*. Eos Trans. AGU, 73, 329.

Ewing, M.A.; Vine, A.C.; and Worzel, J.L. [1946]. *Photography of the ocean bottom*. J. Opt. Soc. Am., 36, 307.

Ferrini, V.L.; Fornari, D.J.; Shank, T.M.; Kinsey, J.C.; Tivey, M.A.; Carbotte, S.M.; Soule, S.A.; Whitcomb, L.L.; Yoerger, D.; and Howland, J. [in press]. *Sub-meter bathymetric mapping of the East Pacific Rise crest at 9°50'N: Linking volcanic and hydrothermal processes*. Geochem. Geophys. Geosyst.

Fornari, D.J.; Humphris, S.E.; Parson, L.M.; Blondel, P.; and German, C.R. [1996]. *Detailed Structure of Lucky Strike Seamount Based on DSL-120 kHz Sonar, ARGO-II and ROV Jason Studies*. Eos Trans. AGU, 77, 699.

Fornari, D.J.; Humphris, S.E.; and Perfit, M.R. [1997]. *Deep submergence science takes a new approach*. Eos Trans. AGU, 78, 402&408.

Fornari, D.; Kurras, G.; Edwards, M.; Spencer, W.; and Hersey, W. [1998]. *Mapping volcanic morphology on the crest of the East Pacific Rise 9° 49'-52'N using the WHOI towed camera system: a versatile new*

digital camera sled for seafloor mapping, BRIDGE Newsletter, 14, 4-12.

Fornari, D.J. [2003]. *A new deep-sea towed digital camera and multi-rock coring System*. Eos, Trans. Am. Geophys. Union, 84, 69&73.

Fornari, D.J.; Tivey, M.A.; Schouten, H.; et al. [2004]. *Submarine Lava Flow Emplacement at the East Pacific Rise 9° 50′N: Implications for Uppermost Ocean Crust Stratigraphy and Hydrothermal Fluid Circulation*. In: The Subsurface Biosphere at Mid-Ocean Ridges, AGU monograph RIDGE Theoretical Institute), W. Wilcock et al., eds., in press, 2004.

Fornari, D.J.; Voegeli, F.; and Olsson, M. [1996]. *Improved low-cost, time-lapse temperature loggers for deep ocean and sea floor observatory monitoring*. RIDGE Events, 7, 13-16.

Fornari, D.J.; Shank, T.M.; Von Damm, K.L.; Gregg, T.K.P.; Lilley, M.; Levai, G.; Bray, A.; Haymon, R.M.; Perfit, M.R.; and Lutz, R.A. Lutz [1998]. *Time-series temperature measurements at high-temperature hydrothermal vents: East Pacific Rise 9°49'N to 9°51'N: monitoring dike intrusion and crustal cracking events*. Earth and Planet. Sci. Lett., 160, 419-431.

Fornari, D.J. and Shank, T.M. [1999]. *Summary of high- and low-T time-series vent fluid temperature experiments East Pacific Rise Vents 9° 49'-51'N*. EXTREME-1 Cruise, May 1999, R/V Atlantis Cruise 03-34, July 1 (cruise report).

Fox, C.G.; Murphy, K.M.; and Embley, R.W. [1988]. *Automated display and statistical analysis of deep-sea bottom photography*. Mar. Geol., 78, 199.

Garry, W.B.; Gregg, T.K.P.; et al. [2006]. *Formation of submarine lava channel textures: insights from laboratory simulations*. Jour. Geophys. Res., 111: doi10.10292005JB003796.

Grassle, J.F.; Berg, C.G.; Childress, J.J.; Grassle, J.P.; Hessler, R.R.; Jannasch, H.J.; Karl, D.M.; Lutz, R.A.; Mickel, T.J.; Rhoads, D.C.; Sanders, H.L.; Smith, K.L.; Somero, G.N.; Turner, R.D.; Tuttle, J.H.; Walsh, P.J.; and Williams, A.J. [1979]. *Galapagos '79 initial findings of a deep-sea biological quest*. Oceanus, 22, 2.

Heezen, B.C. and Hollister, C.D. [1971]. *The face of the deep*. 659 pp., Oxford University Press, New York.

Hey, R.N.; Kleinrock, M.C.; Martinez, F.; et al. [1998]. *High-resolution mapping and imaging of the fastest seafloor spreading system*. Eos, Am. Geophys. U.

Hey, R.; Baker E.; et al. [2004]. *Tectonic/volcanic segmentation and controls on hydrothermal venting along Earth's fastest seafloor spreading system, EPR 27°–32°S*. Geochem. Geophys. Geosyst., 5, Q12007, doi:10.1029/2004GC000764.

Howland, J.C. [1998]. *Imagery collection and mosaicking, Derbyshire Survey 1997*. Proceedings MTS/Ocean Community Conference '98, Vol. 2, pp. 1104-1108, Baltimore, Maryland, November.

Howland, J.C.; Singh, H.; Marra, M.; and Potter, D. [1999]. *Digital mosaicking of underwater imagery*. Sea Technology, pp. 65-69, June.

Humphris, S.E. and Kleinrock, M.C. [1996]. *Detailed morphology of the TAG active hydrothermal mound: Insights into its formation and growth*. Geophys. Res. Lett., 23: 3443-3446.

Humphris, S.E.; Fornari, D.J.; and Scheirer, D.S. [2002]. *Geotectonic setting of hydrothermal activity on the summit of Lucky Strike Seamount (37° 17'N, Mid-Atlantic Ridge)*. Geochem. Geophys. Geosyst., 3, 10.1029/2001GC000284.

Karson, J.A.; Klein, E.M.; Hurst, S.D.; et al. [1999]. *Hess Deep '99- A DSL-120, ARGO II, and Alvin study of upper crustal structure at the Hess Deep Rift: a new look at fast-spread crust of the EPR*. Cruise Report.

Karson, J.; Kelley, D.; Fornari, D.; Perfit, M.; and Shank, T. [2015]. *Discovering the deep: a photographic atlas of the seafloor and ocean crust*. Cambridge U. Press.

Kim, S.L. and Mullineaux, L.S. [1998]. *Distribution and near-bottom transport of larvae and other plankton at hydrothermal vents*. Deep-Sea Research II, 45: 423-440.

Kleinrock, M.C. and Humphris, S.E. [1996]. *Structural controls on the localization of hydrothermalism at the TAG active mound, Mid-Atlantic Ridge 26˚N*. Nature, 382, 149-153.

Kurras, G.; Fornari, D.J.; and Edwards, M.H. [2000]. *Volcanic morphology of the East Pacific Rise crest 9°49'-52'N: implications for extrusion at fast spreading mid-ocean ridges*. Mar. Geophys. Res., 21, 23-41.

Langmuir, C.H.; Humphris, S.E.; Fornari, D.; Van Dover, C.L.; Von Damm, K.; Tivey, M.K.; Colodner, D.; Charlou, J.L.; Desonie, D.; Wilson, C.; Fouquet, Y.; Klinkhammer, G.; and Bougault, H. [1995]. *Description and significance of hydrothermal vents near a mantle hot spot: the Lucky Strike vent field at 37°N, Mid-Atlantic Ridge*. Earth Planet. Sci. Lett., 148, 69-91.

Lerner, S.; Howland, J.; Humphris, S.; and Lange, W. [1996]. *Interactive inspection and analysis of multi-sensor data from the TAG hydrothermal vent site*. Eos, Trans. of the Am. Geophys. Union, 77, p. 768.

Lonsdale, P. and Spiess, F.N. [1980]. *Deep-tow observations at the East Pacific Rise, 8˚45'N, and some interpretations*. Initial Rep. Deep Sea Drill. Proj., 54, 43.

McDermott, J.M.; Parnell-Turner, R.; Barreyre, T.; Herrera, S.; Downing, C.; Pittors, N.; Vohsen, S.; Dowd, W.; Wu, J-N.; Marjanovic, M.; and Fornari, D.J. [2022]. *Discovery of active off-axis hydrothermal vents at 9° 54'N East Pacific Rise*. PNAS, 119 (30), e2205602119 https://doi.org/10.1073/pnas.220560 2119.

Mullineaux, L.S.; Mills, S.W.; and Goldman, E. [1998]. *Recruitment variation during a pilot colonization study of hydrothermal vents (9°50'N, East Pacific Rise)*. Deep-Sea Research II 45:441-464.

RIDGE2000 Program Plan [2004]. Available at: http://ridge2000.org.

Sarrazin, J.; Robigou, V.; Juniper, S.K.; and Delaney, J.R. [1997]. *Biological and geological dynamics over four years on a high-temperature sulfide structure at the Juan de Fuca Ridge hydrothermal observatory*. Mar. Ecol. Prog. Ser., 153, 5-24.

Sarrazin, J. and Juniper, S.K. [1999]. *Biological characteristics of a hydrothermal edifice mosaic community*. Mar. Ecol. Prog. Ser.

Scheirer, D.S.; Fornari, D.J.; Humpris, S.E.; and Lerner, S. [2000]. *High-resolution seafloor mapping using the DSL-120 sonar system: quantitative assessment of sidescan and phase-bathymetry data from the Lucky Strike segment of the Mid-Atlantic Ridge*. Mar. Geophys. Res., 21, 121-142.

Scheirer, D.S.; Shank, T.M.; and Fornari, D.J. [2006]. *Temperature variations at diffuse and focused flow hydrothermal vent sites along the Northern East Pacific Rise, 7, 3, Q03002*. Geochem. Geophys. Geosyst., doi:10.1029/2005GC001094.

Shank, T.M.; Scheirer, D.S.; and Fornari, D. [2001]. *Time series studies of faunal colonization and temperature variations at diffuse-flow hydrothermal vent sites near 9°50'N, EPR*. Eos Trans. AGU, 82, 196.

Shank, T.M.; Fornari, D.J.; Von Damm, K.L.; Lilley, M.D.; Haymon, R.M.; and Lutz, R.A. [1998]. *Temporal and spatial patterns of biological community development at nascent deep-sea hydrothermal vents along the East Pacific Rise, 9° 49.6'N - 9° 50.4'N*. Deep Sea Research, II, 45, 465-515.

Shank, T.M.; Fornari, D.J.; et al. [2003]. *Deep submergence synergy: Alvin and ABE explore the Galapagos Rift at 86°W*. Eos, Trans. American Geophys. Union, 84, 425, 432-433.

Singh, H.; Howland, J.; Duester, A.; Bradley, A.; and Yoerger, D. [1996]. *Quantitative stereo imaging from the autonomous benthic explorer (ABE)*. Presented at the Symposium on Autonomous Underwater Vehicle Technology, Monterey, California.

Singh, H.; Howland, J.; Yoerger, D.; and Whitcomb, L. [1998]. *Quantitative photomosaicking of underwater imagery*. Proceedings Oceans '98, IEEE/OES Conference, Nice, France, Vol. 1, pp. 263-266, September/October.

Singh, H.; et al. [2004]. *Seabed AUV offers new platform for high-resolution imaging*. Eos, Trans. American Geophys. Union, 85, 289, 294-295.

Sinton, J.; Bergmanis, E.; Rubin, K.H.; et al. [2002]. *Volcanic eruptions on mid-ocean ridges: new evidence from the superfast spreading East Pacific Rise 17˚-19˚S*. Jour. Geophys. Res., 107(B6): 21.

Sohn, R.A.; Fornari, D.; Von Damm, K.L.; Hildebrand, J.A.; and Webb, S.C. [1998]. *Seismic and hydrothermal evidence for a cracking event on the East Pacific Rise crest at 9°50'N*. Nature, 396, 159-161.

Sohn, R.A.; Hildebrand, J.A.; and Webb, S.C. [1999]. *A microearthquake survey of the high-temperature vent fields on the volcanically active East Pacific Rise*. J. Geophys. Res., 104 (11), 25,367-25,378.

Sohn, R.A.; Humphris, S.A.; and Canales, J. [2005]. *Stochastic analysis of exit-fluid temperature time-series data from the TAG hydrothermal mound: events, states, and hidden Markov models*. Am. Geophys. Union, Eos, 86(52), OS22A-06.

Soule, S.A.; Fornari, D.J; et al. [2005]. *Channelized lava flows at the East Pacific Rise crest 9-10˚N: the importance of off-axis lava transport in developing the architecture of young oceanic crust*. Geochem. Geophys. Geosyst., 6(8): doi:10.1029/2005GC000912.

Spiess, F.N. and Tyce, R.C. [1973]. *Marine Physical Laboratory deep tow instrumentation system*, ref. 73-4. Scripps Inst. Oceanogr., Lab Jolla, Calif.

Sulanowska, M.M.; Humprhis, S.E.; Howland, J.C.; and Kleinrock, M.C. [1996]. *Detailed analysis of the surface morphology of the active TAG hydrothermal mound by mosaicking of digital images*. Eos, Trans. of the American Geophysical Union, Eos, 77, 768.

Tolstoy, M.; Cowen, J.P.; Baker, E.T.; Fornari, D.J.; Rubin, K.H.; Shank, T.M.; Waldhauser, F.; Bohnenstiehl, D.R.; Forsyth, D.W.; Holmes, R.C.; Love, B.; Perfit, M.R.; and Weekly, R.T. [2006]. *A seafloor spreading event captured by seismometers: forecasting and characterizing an eruption*. Science, DOI: 10.1126/science.1133950.

Trask, J. and Van Dover, C.L. [1999]. *Site-specific and ontogenetic variations in nutrition of mussels (Bathymodiolus sp.) from the Lucky Strike hydrothermal vent field, Mid-Atlantic Ridge*. Limnology and Oceanography, 44, 334-343.

Van Dover, C.L.; Trask, J.; Gross, J.; and Knowlton, A. [1999]. *Reproductive biology of free-living and commensal polynoid polychaetes at the Lucky Strike hydrothermal vent field (Mid-Atlantic Ridge)*. Marine Ecology Progress Series.

Wu, J.; Parnell-Turner, R.E.; Fornari, D.J.; Kurras, G.; Berrios-Rivera, N.; Barreyre, T.; and McDermott, J.M. [2022]. *Extent and volume of lava flows erupted at 9°50'N, East Pacific Rise in 2005-2006 from autonomous underwater vehicle surveys*. Geochemistry, Geophysics, Geosystems, 23(3), 1-35. https://doi.org/10.1029/2021gc010213.

Yoerger, D.; Singh, H.; Whitcomb, L.; Mindell, D.; Adams, J.; Foley, B.; and Catteati, J. [1988]. *Precise optical and acoustic mapping of the Skerki Bank Wrecks using the Jason ROV*. Society for Historical Archaeology – Conference on Historical and Underwater Archaeology, Atlanta, Georgia, January.

Yoerger, D.R.; Bradley, A.M.; Cormier, M-H.; Ryan, W.B.F.; and Walden, B.B. [1999]. *High resolution mapping of a fast spreading Mid Ocean Ridge with the autonomous benthic Explorer*. 11th International Symposium on Unmanned Untethered Submersible Technology (UUST99), Durham, New Hampshire, August.

Yoerger, D.R.; Kelley, D.S.; and Delaney, J.R. [1999]. *Fine-scale three-dimensional mapping of a deep-sea hydrothermal vent site using the Jason ROV system*. International Conference on Field and Service Robotics (FSR '99), Pittsburgh, Pennsylvania, August.

YouTube links

Compiled video footage from Expedition AT50-21 in 2024 at the East Pacific Rise 9° 46'-54'N showing primarily MISO GoPro 5.3K video as well as DeepSea 4K video from *Alvin's* Optim cameras
https://www.youtube.com/watch?v=VlLYU25VfII

Compiled video footage from Expedition AT50-09 in 2023 in the Galápagos Marine Reserve showing primarily MISO GoPro 5.3K video as well as DeepSea 4K video from *Alvin's* Optim cameras
https://www.youtube.com/watch?v=sa3J-0sMUjo

Compiled video footage from Expedition AT42-06 in 2018 at the East Pacific Rise 9° 50'N showing primarily MISO GoPro 4K video as well as DeepSea 4K video from *Alvin's* Optim cameras
https://www.youtube.com/watch?v=7dYVPtFCWQ4